*GEOLOGICA CARPATHICA*, DECEMBER 2013, 64, 6, 419–435 doi: 10.2478/geoca-2013-0029

# Geochronology and petrogenesis of granitoid rocks from the Goryczkowa Unit, Tatra Mountains (Central Western Carpathians)

JOLANTA BURDA[1]✉, ALEKSANDRA GAWĘDA[1] and URS KLÖTZLI[2]

[1]University of Silesia, Faculty of Earth Sciences, Będzińska 60, 41-200 Sosnowiec, Poland;
✉jolanta.burda@us.edu.pl; aleksandra.gaweda@us.edu.pl
[2]University of Vienna, Department of Lithospheric Research, Althanstrasse 14, 1090 Vienna, Austria; urs.kloetzli@univie.ac.at

*(Manuscript received January 7, 2013; accepted in revised form October 16, 2013)*

**Abstract:** The geochemical characteristics as well as the LA-MC-ICP-MS U-Pb zircon age relationship between two granitoid suites found in the Goryczkowa crystalline core in the Western Tatra Mountains were studied. The petrological investigations indicate that both granitoid suites were emplaced at medium crustal level, in a VAG (volcanic arc granites) tectonic setting. However, these suites differ in source material melted and represent two different magmatic stages: suite 1 represents a high temperature, oxidized, pre-plate collision intrusion, emplaced at ca. 371 Ma while suite 2 is late orogenic/anatectic magma, which intruded at ca. 350 Ma. These data are consistent with a period of intensive magmatic activity in the Tatra Mountain crystalline basement. The emplacement of granitoids postdates the LP-HT regional metamorphism/partial melting at ca. 387 Ma and at 433–410 Ma, imprinted in the inherited zircon cores.

**Key words:** Western Carpathians, Tatra Mountains, U-Pb zircon geochronology, Goryczkowa granitoids.

## Introduction

The crystalline basement of the Tatra Mountains is one of several Variscan crystalline complexes in the Central Western Carpathians (CWC; Fig. 1a). The granitoid rocks, which are the most important constituents of the Tatra Mountains crystalline core, have intruded a series of metamorphic rocks (e.g. Gawęda et al. 2000; Burda & Klötzli 2011). The origin of this magmatism is related to continent–continent collision during the Devonian and Carboniferous (e.g. Poller et al. 2000, 2001; Burda et al. 2011). In spite of recent U-Pb zircon age dating many uncertainties persist regarding the origin, development and timing of the granitoid magma batches. The still unsolved problem is the origin and age of the so-called Goryczkowa granitoids.

The granitoids form a main portion of the Goryczkowa Unit, representing a fragment of the crystalline core, displaced during the Alpine folding and thrusting event, which formed the Carpathian arc. At present, crystalline fragments form three cores of the Giewont Nappe in the northern part of the Tatra massif (Fig. 1c). Accessible WR (whole rock) Rb-Sr isochron data pointed to an age of 300–290 Ma for granitoid rocks emplacement while the Goryczkowa gneisses yielded an Rb-Sr isochron age of 413 ± 10 Ma (Burchart 1968).

The main purpose of this study is to discuss the petrogenesis and zircon U-Pb ages of two types of Goryczkowa granitoids. As a result we verify the currently published opinions about the petrological and classification autonomy of the Goryczkowa granitoids. In order to better constrain the emplacement ages, inter-relations and evolution of these granitoids, field observations, major and trace element chemistry and LA-MC-ICP-MS (Laser Ablation Multi-Collector Inductively Coupled Plasma Mass Spectrometry) U-Pb zircon age calculations were combined with studies of zircon morphology and internal structures. The results are compared with published petrological data and time constraints. The inherited components, present in granitoid rocks are also discussed to understand the trace element signatures of both granitoid suites.

## Geological setting

The crystalline basement of the Tatra Mountains is one of several crystalline basement units in the Alpine belt of the Central Western Carpathians. It comprises polygenetic Variscan granitoids that are volumetrically predominant and an early Variscan migmatitic metamorphic envelope (e.g. Gawęda 2001; Burda & Gawęda 2009; Burda & Klötzli 2011).

In the polygenetic granitoid pluton four petrographic types of granitoids were distinguished (Kohút & Janák 1994). The common Tatra granodiorite-tonalite forms a volumetrically predominant tongue-shaped intrusion, dated at 368–350 Ma (Poller et al. 2000, 2001; Burda et al. 2011). Quartz-diorites (I-type mingled hybrid, interpreted as magmatic precursors) are present as sills inside the metamorphic envelope, in the border zone of the common Tatra granite (Gawęda et al. 2005). The mingling-mixing processes between the common Tatra type and quartz-diorite precursors were dated to 368 ± 8 Ma (Burda et al. 2011). The High Tatra granite (I/S-type) predominates in the eastern part of the massif (Fig. 1b) and is characterized by the abundance of mafic enclaves and xenoliths of country rocks (Gawęda 2009). Published zircon U-Pb data suggest an emplacement age of

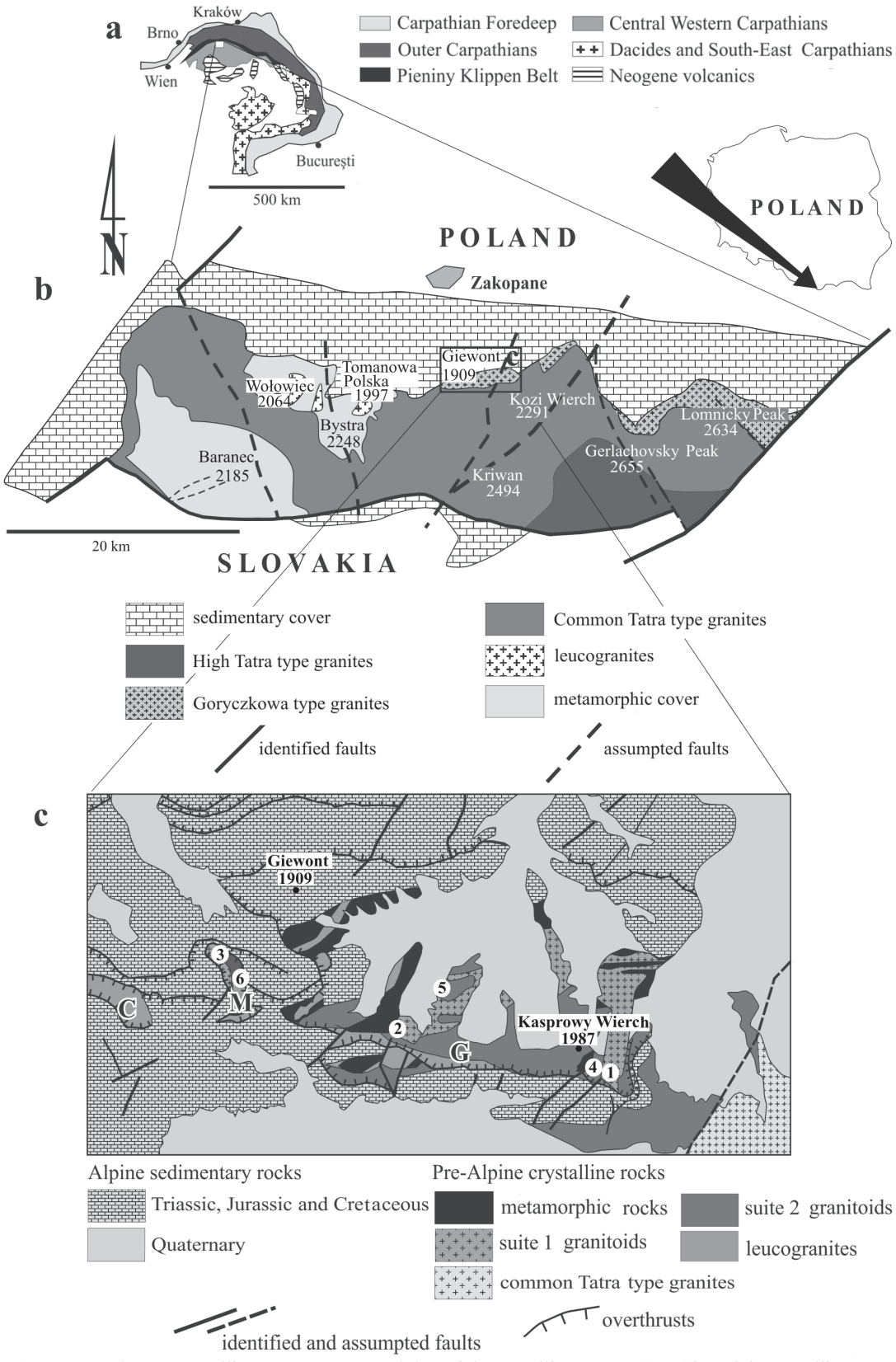


**Fig. 1.** The geology of the Tatra Mountains: **a** — simplified geological sketch of the Carpathian chain; **b** — geological map of the Tatra Mountains Block (after Kohút & Janák 1994; Bac-Moszaszwili 1996; Gawęda et al. 2005); **c** — simplified geological map of the study area in the northern part of the Tatra crystalline basement (Giewont Nappe) with sample locations.

345–335 Ma (Gawęda 2008; Burda 2010; Burda et al. 2013). The age of the mafic microgranular enclaves (341 Ma; Poller et al. 2001) falls into this range.

Goryczkowa-type granitoids were distinguished in the northern part of the Goryczkowa crystalline core (Fig. 1b) as the grey biotite monzogranite with oriented fabric (Morozewicz 1914; Kohút et al. 2009), associated with pink, porphyritic leucocratic granites (Fig. 2a). The age of both granites remains largely imprecise, ranging from 300–290 Ma (Burchart 1968), 365–353 Ma (Kohút & Siman 2011) to 356 ± 8 Ma for leucocratic granite (Burda & Klötzli 2007).

The crystalline complex is covered by nappes of Mesozoic sedimentary rocks, which also include fragments of the crystalline basement (Fig. 1b,c). One of these nappes is the Giewont Nappe (Jurewicz 2006 and references therein), which was formed by overthrusting of the sedimentary rocks, together with the underlying crystalline basement, now present as the crystalline cores of the nappe. These cores are exposed in Goryczkowa, Małołączniak and Ciemniak Units (Fig. 1c). They comprise metamorphic rocks, leucogranites (called alaskites) associated with migmatites (Jaroszewski 1965; Burchart 1968) and interpreted as the effects of accretionary prism partial melting (Gawęda 2001), comparable with those found in the Western Tatra Mountains (ca. 360 Ma; Gawęda 2001; Burda & Gawęda 2009) and two suites of granitoid rocks: granodiorite-tonalite, called Goryczkowa type granitoids and muscovite alkali-feldspar granites (Burchart 1968, 1970). For the latter, preliminary U-Pb zircon dating pointed to an intrusion age of 356 ± 8 Ma (Burda & Klötzli 2007).

## Analytical methods

Rock samples weighing about 25 kg were collected from the two main varieties of granitoids from the Goryczkowa and Małołączniak crystalline cores (Fig. 1c).

Whole-rock samples were analysed by ICP-ES (Inductively Coupled Plasma Emission Spectrometer) for major and LILE (large-ion lithophile) trace elements and by ICP-MS (Inductively Coupled Plasma Mass Spectrometry) for HFSE (high field strength elements) and REE in the ACME Analytical Laboratories, Vancouver, Canada, using sets of internationally accepted standards, according to procedures described on http://acmelab.com. REEs are normalized to C1 chondrite (Sun & McDonough 1989).

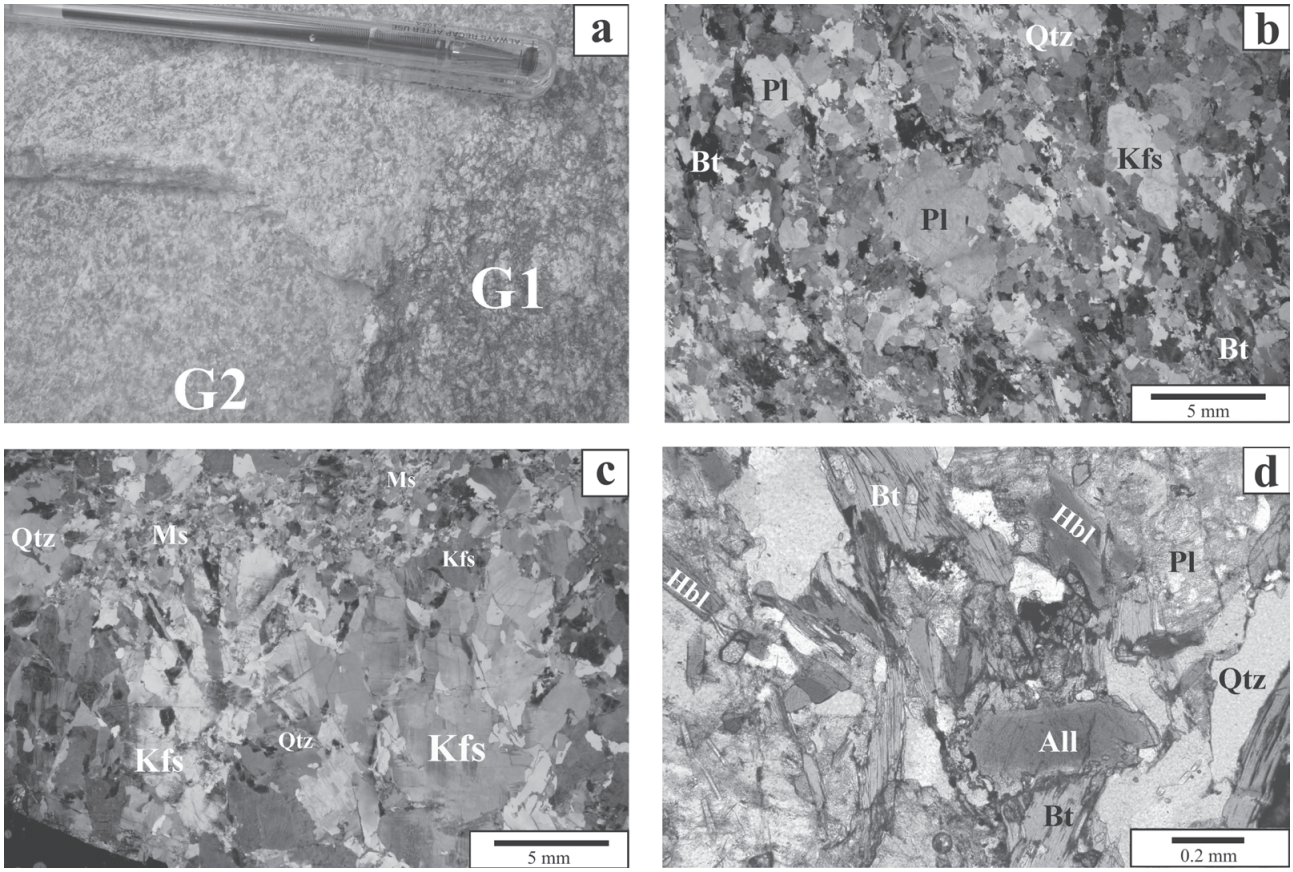


**Fig. 2.** Photographs of the granitoids from the Goryczkowa crystalline core: **a** — equigranular biotite granodiorite (sample G1 — suite 1) and alkali-feldspar granite (sample G2 — suite 2). The length of the pen is 10 cm; **b** — oriented texture of biotite granodiorite (suite 1); **c** — porphyritic alkali feldspar granite (suite 2) with a fragment of the alkali feldspar porphyrocryst showing the internal graphic intergrowths with quartz, flowing in the muscovite-quartz-feldspar groundmass; **d** — allanite crystal in amphibole-bearing monzogranite (suite 1). Abbreviations: **Pl** — plagioclase, **Kfs** — K-feldspar, **Qtz** — quartz, **Bt** — biotite, **Ms** — muscovite, **Hbl** — hornblende, **All** — allanite.

Microprobe analyses of main and accessory minerals were carried out in the Inter-Institution Laboratory of Microanalyses of Minerals and Synthetic Substances, Warsaw (CAMECA SX-100 electron microprobe; 15 kV, 20 nA, 4 s counting time for peak and background, 1–5 μm beam diameter), using sets of internationally recognized natural and synthetic standards.

Mineral abbreviations used here follow those proposed by Whitney & Evans (2010). Zircon crystals from both granitoid suites (samples G1 and G2 collected from the top of Beskid) were separated using standard techniques (crushing, hydrofracturing, washing, Wilfley shaking table, Frantz magnetic separator and handpicking). The separation was carried out in the Institute of Geological Sciences, Polish Academy of Sciences, Cracow. Zircon grains were selected for morphological study using scanning electron microscopy and then imaged by panchromatic cathodoluminescence using a FET Philips 30 electron microscope (15 kV and 1 nA) at the Faculty of Earth Sciences, University of Silesia, Sosnowiec. Zircon $^{206}Pb/^{238}U$ and $^{207}Pb/^{206}Pb$ ages were determined using a 193-nm solid state Nd-YAG (neodymium-yttrium aluminium garnet) laser coupled to a Nu PLASMA HR multi collector ICP mass spectrometer in the Geochronology Laboratory, Institute of Geology at the University of Vienna. Ablation in a He atmosphere was either spot- or raster-wise according to the zircon CL zonation patterns. Spot analyses were 15–25 μm in diameter whereas rastering line widths were 10–15 μm with a rastering speed of 5 μm/sec. The calculated intercept values were corrected for mass discrimination by reference to measurements of the zircon standard Plesovice (337.13 ± 0.37 Ma; Sláma et al. 2008) made during the analytical session. The final U/Pb ages were calculated with 2σ errors using the Isoplot/Ex version 3.00 program (Ludwig 2003). Details of analytical procedures and data reduction schemes are given in Klötzli et al. (2009).

## Petrography and mineral chemistry

The granitoids of the Goryczkowa can be subdivided into two main suites (Fig. 2a; Burchart 1970). Representative samples of both suites were collected from the Beskid Mt, Goryczkowa Czuba and Świńska Valley, all located in the so-called Goryczkowa and Małołączniak crystalline cores of the Giewont Nappe (Fig. 1c).

Suite 1 is represented by biotite granodiorite, amphibole-biotite tonalite and quartz-diorite (Fig. 2), traditionally called Goryczkowa type granitoids (Morozewicz 1914; Kohút et al. 2009). It is the most abundant granitoid type of Goryczkowa crystalline core. Biotite granodiorite is a medium-grained rock with oriented texture and typical plagioclase "augen" coated by biotite and amphibole (Fig. 2b). The main mineral components are plagioclase porphyrocrysts showing oscilatory zonation ($An_{32-12}$), quartz, biotite (***#fm*** = 0.555–0.557, Ti = 0.346–0.436 a.p.f.u.; Table 1), amphibole (Mg-hornblende; Table 2), K-feldspar ($Or_{88-91}Ab_{10-6}Cn_{2-3}$). Apatite, zircon, Ti-magnetite and monazite-(Ce) are present as accessories. The amphibole-biotite tonalite and quartz-diorite are composed of plagioclase ($An_{45-62}$), amphibole, biotite

**Table 1:** Micro-chemical compositions and crystal chemical formulae of micas from both granitoid suites. Explanations: ***#fm*** = (Fe + Mn)/(Fe + Mn + Mg); **MsC** — muscovite core; **MsM** — muscovite margin.

| **Sample** | **Suite 1** | | | | | | **Suite 2** | |
|---|---|---|---|---|---|---|---|---|
| **Component** | **Bt1-G4** | **Bt2-G4** | **Bt3-G1** | **Bt4-G1** | **MsC-G1** | **MsM-G1** | **Ms1-G2** | **Ms2-G2** |
| $SiO_2$ | 37.18 | 36.70 | 35.82 | 35.75 | 45.67 | 45.58 | 48.01 | 46.08 |
| $TiO_2$ | 2.62 | 3.18 | 3.00 | 3.81 | 0.63 | 0.49 | 0.04 | 0.43 |
| $Al_2O_3$ | 16.05 | 15.23 | 16.65 | 17.08 | 33.38 | 33.19 | 33.86 | 32.83 |
| $Cr_2O_3$ | 0.01 | 0.06 | 0.03 | 0.02 | – | – | – | – |
| $V_2O_5$ | 0.15 | 0.18 | 0.02 | 0.04 | – | – | – | – |
| MgO | 13.58 | 13.30 | 9.43 | 9.23 | 1.02 | 0.81 | 1.21 | 1.31 |
| MnO | 0.23 | 0.20 | 0.24 | 0.27 | – | 0.04 | 0.00 | 0.05 |
| FeO | 15.67 | 16.41 | 20.69 | 19.83 | 3.57 | 4.03 | 1.77 | 3.52 |
| BaO | – | – | – | – | – | – | 0.12 | 0.13 |
| $Na_2O$ | 0.08 | 0.11 | 0.11 | 0.11 | – | – | – | – |
| $K_2O$ | 9.53 | 9.82 | 9.79 | 9.69 | 10.74 | 10.73 | 10.87 | 11.00 |
| $H_2O_{calc}$ | 4.00 | 3.96 | 3.91 | 3.94 | 4.37 | 4.42 | 4.52 | 4.35 |
| F | – | – | – | – | 0.12 | – | 0.02 | 0.31 |
| Total | 99.10 | 99.15 | 99.69 | 99.77 | 99.50 | 99.29 | 100.42 | 100.01 |
| **Crystal-chemical formula calculated for 22 $O^{2-}$** | | | | | | | | |
| Si | 5.578 | 5.552 | 5.489 | 5.445 | 6.178 | 6.188 | 6.356 | 6.273 |
| $Al^{IV}$ | 2.422 | 2.448 | 2.511 | 2.555 | 1.822 | 1.812 | 1.644 | 1.727 |
| $Al^{VI}$ | 0.416 | 0.267 | 0.496 | 0.51 | 3.498 | 3.498 | 3.639 | 3.464 |
| Ti | 0.295 | 0.361 | 0.346 | 0.436 | 0.064 | 0.05 | 0.004 | 0.043 |
| V | 0.015 | 0.018 | 0.002 | 0.005 | – | – | – | – |
| Cr | 0.002 | 0.007 | 0.003 | 0.002 | – | – | – | – |
| Mg | 3.037 | 2.999 | 2.154 | 2.035 | 0.206 | 0.164 | 0.238 | 0.261 |
| Mn | 0.029 | 0.023 | 0.031 | 0.035 | – | 0.005 | – | 0.006 |
| Fe | 1.966 | 2.077 | 2.652 | 2.526 | 0.404 | 0.457 | 0.195 | 0.393 |
| Ba | – | – | – | – | – | – | 0.006 | 0.007 |
| Na | 0.023 | 0.032 | 0.033 | 0.032 | – | – | – | – |
| K | 1.824 | 1.918 | 1.914 | 1.884 | 1.853 | 1.858 | 1.836 | 1.872 |
| ***#fm*** | 0.396 | 0.412 | 0.555 | 0.557 | 0.662 | 0.730 | 0.450 | 0.595 |

(#*fm* = 0.396–0.414 and Ti = 0.295–0.361 a.p.f.u.; Table 1), quartz, allanite-epidote and titanite. Amphibole is represented by tchermakite, tchermakitic-hornblende, ferrian-magnesio-hornblende to magnesio-hornblende, locally overgrown by secondary actinolite-tremolite (Table 2). Epidotes show normal zonation from allanite cores to REE-epidote on the rims (Table 3), which is typical of high-pressure magmatic epidote (Schmidt & Poli 2004). K-feldspar is present as a minor component. Accessories are represented by Ti-magnetite–ilmenite, zircon, and apatite. Secondary minerals are represented by zoned post-magmatic muscovite (#*fm* = 0.662–0.730; Ti = 0.064–0.050 a.p.f.u.; Table 1) epidote and titanite.

The granitoids of suite 2 are leucocratic porphyritic alkali-feldspar granites, showing cross-cutting relations to the Goryczkowa type granitoid rocks (Fig. 2a). The most pronounced feature of these granites is the presence of large (up to 2 cm in length) crystals of pink perthitic alkali feldspars, showing internal graphic intergrowths with quartz, all flowing in a medium- to coarse-grained matrix of plagioclase ($An_{7-13}$), K-feldspar ($Or_{97}Ab_3$–$Or_{93}Ab_7$), quartz and abundant muscovite (Fig. 2c). Accessory phases comprise apatite, zircon and monazite-(Ce). Muscovite is chemically zoned, with $TiO_2$ content in the range of 0.43–0.04 (0.040–0.004 a.p.f.u.) and #*fm* = 0.450–0.595 (Table 1).

## Geochemistry and geotectonic interpretation

The granodiorite–tonalite–quartz-diorite rocks (suite1) are peraluminous (ASI = 1.11–1.26) with silica contents around 63–70 wt. %, calc-alkaline (Fig. 3a), characterized by $Na_2O > K_2O$ and low Rb/Sr ratio = 0.05–0.12. In the Frost & Frost (2008) geochemical classification these rocks belong to the magnesian family (Fig. 3b). The chondrite-normalized (Sun & McDonough 1989) REE patterns show moderate LREE enrichment ($Ce_N/Yb_N$ = 18.12–24.18) while an Eu anomaly is almost absent (Eu/Eu* = 0.82–1.00; Table 4, Fig. 4). Temperatures calculated on the basis of Zr-geothermometer of Watson & Harrison (1983) for these rocks are in the range of 767–803 °C (Table 4).

**Table 2:** Chemical composition and crystal-chemical formulae of primary (**Amph**) and secondary (**Trem–Act**) amphibole crystals.

| **Component [wt. %]** | **Amph 1** | **Amph 2** | **Amph 3** | **Trem 1** | **Act 1** |
|---|---|---|---|---|---|
| $SiO_2$ | 44.16 | 43.69 | 44.36 | 51.45 | 54.71 |
| $TiO_2$ | 0.83 | 0.96 | 0.60 | 0.01 | 0.05 |
| $Al_2O_3$ | 10.59 | 10.99 | 10.62 | 2.82 | 0.89 |
| $Cr_2O_3$ | 0.00 | 0.02 | 0.03 | 0.00 | 0.02 |
| FeO | 16.14 | 16.11 | 15.27 | 13.76 | 13.86 |
| MnO | 0.50 | 0.52 | 0.41 | 0.45 | 0.68 |
| MgO | 11.33 | 11.06 | 11.97 | 16.09 | 14.55 |
| CaO | 11.77 | 11.72 | 10.83 | 10.46 | 12.12 |
| $Na_2O$ | 1.00 | 1.16 | 0.85 | 0.22 | 0.40 |
| $K_2O$ | 0.77 | 0.83 | 0.60 | 0.06 | 0.07 |
| F | 0.21 | 0.20 | 0.17 | 0.00 | 0.00 |
| Cl | 0.07 | 0.06 | 0.07 | 0.00 | 0.00 |
| $H_2O$amp | 1.80 | 1.78 | 1.78 | 2.02 | 2.06 |
| $Fe_2O_3$ (calc) | 4.37 | 6.42 | 10.74 | 13.69 | 0.78 |
| FeO | 9.74 | 10.33 | 5.60 | 1.44 | 13.16 |
| O=F,Cl | –0.11 | –0.10 | –0.09 | 0.00 | 0.00 |
| Total | 99.75 | 99.64 | 98.55 | 98.99 | 99.36 |
| **Formula per 23 $O^{2-}$ (13 cations)** | | | | | |
| Si | 6.518 | 6.471 | 6.530 | 7.378 | 7.932 |
| Al $^{IV}$ | 1.482 | 1.529 | 1.470 | 0.476 | 0.068 |
| Al $^{VI}$ | 0.360 | 0.388 | 0.372 | 0.000 | 0.083 |
| Ti | 0.092 | 0.107 | 0.066 | 0.001 | 0.006 |
| Cr | 0.000 | 0.002 | 0.003 | 0.000 | 0.002 |
| $Fe^{3+}$ | 0.784 | 0.716 | 1.190 | 1.478 | 0.085 |
| $Fe^{2+}$ | 1.208 | 1.279 | 0.690 | 0.173 | 1.596 |
| Mn | 0.062 | 0.065 | 0.051 | 0.055 | 0.084 |
| Mg | 2.494 | 2.442 | 2.627 | 3.439 | 3.145 |
| Ca | 1.862 | 1.860 | 1.708 | 1.608 | 1.882 |
| Na | 0.287 | 0.333 | 0.243 | 0.062 | 0.111 |
| K | 0.144 | 0.157 | 0.113 | 0.010 | 0.013 |
| (Na+K) (A) | 0.293 | 0.350 | 0.113 | 0.010 | 0.013 |
| $Mg/(Mg+Fe^{+2})$ | 0.674 | 0.656 | 0.792 | 0.952 | 0.663 |
| $Fe^{+3}/(Fe^{+3}+Al^{VI})$ | 0.685 | 0.648 | 0.762 | 1.000 | 0.505 |
| **Species** | **Mg-Hbl** | **Tschermakite** | **Mg-Hbl** | **Ferri-tremolitic Hbl** | **Actinolite** |
| T (°C) | 873 | 885 | 865 | 605 | 618 |
| uncertainty ($\sigma_{est}$) | 22 | 22 | 22 | 30 | 34 |
| P(S) [kbar] | 5.8 | 6.1 | 5.8 | – | – |
| ΔNNO | 0.70 | 0.5 | 1.1 | – | – |
| $logfO_2$ | –11.70 | –11.60 | –11.4 | – | – |
| uncertainty ($\sigma_{est}$) | 0.4 | 0.4 | 0.4 | – | – |
| $H_2O_{melt}$ [wt. %] | 7.80 | 7.8 | 8.1 | – | – |

**Table 3:** Representative microanalyses and crystal-chemical formulae (25 $O^{2-}$) of magmatic epidote-allanite and secondary REE-epidote minerals.

| | Magmatic epidote–allanite (Fig. 4c) | | | | Secondary REE-epidote (Fig. 6c) | | | |
|---|---|---|---|---|---|---|---|---|
| | #1 | #2 | #3 | #4 | #1 | #2 | #3 | #4 |
| $SiO_2$ | 33.02 | 32.81 | 32.64 | 32.72 | 32.84 | 36.16 | 33.64 | 37.71 |
| $P_2O_5$ | 0.01 | 0.19 | 0.07 | 0.08 | – | 0.12 | – | 0.11 |
| $TiO_2$ | 1.19 | 0.99 | 0.87 | 0.66 | 0.35 | 0.31 | 1.78 | 0.07 |
| $ThO_2$ | – | 0.43 | 0.53 | 1.11 | 0.47 | 0.16 | 0.03 | – |
| $UO_2$ | 0.06 | – | 0.06 | – | 0.07 | – | – | – |
| $Al_2O_3$ | 16.00 | 17.49 | 17.81 | 17.86 | 18.21 | 22.46 | 8.98 | 23.64 |
| $V_2O_3$ | 0.05 | 0.10 | 0.03 | 0.06 | 0.07 | 0.07 | 0.22 | 0.06 |
| $Fe_2O_3$ | 16.73 | 13.57 | 13.46 | 12.66 | 12.77 | 12.97 | 17.33 | 12.92 |
| $Y_2O_3$ | 0.01 | 0.03 | 0.02 | 0.03 | 0.13 | 0.06 | – | – |
| $La_2O_3$ | 3.63 | 4.66 | 4.14 | 3.39 | 2.42 | 0.51 | 0.04 | 0.06 |
| $Ce_2O_3$ | 8.58 | 8.25 | 8.24 | 7.24 | 6.74 | 1.55 | – | 0.05 |
| $Pr_2O_3$ | 1.08 | 0.56 | 0.68 | 0.71 | 1.13 | 0.15 | – | – |
| $Nd_2O_3$ | 3.07 | 2.81 | 2.84 | 3.38 | 4.36 | 1.18 | – | 0.05 |
| $Sm_2O_3$ | 0.19 | 0.47 | 0.14 | 0.34 | 0.44 | 0.17 | – | 0.05 |
| $Gd_2O_3$ | 0.22 | 0.07 | 0.19 | 0.13 | 0.34 | 0.01 | 0.15 | 0.02 |
| MgO | 0.49 | 1.08 | 1.01 | 0.88 | 0.87 | 0.14 | 0.04 | 0.04 |
| CaO | 13.63 | 14.26 | 14.44 | 14.76 | 14.60 | 20.48 | 35.10 | 23.16 |
| MnO | 0.22 | 0.25 | 0.31 | 0.25 | 0.31 | 0.33 | 0.22 | 0.21 |
| $Na_2O$ | 0.01 | – | 0.02 | 0.08 | 0.06 | – | 0.02 | 0.01 |
| $H_2O_{calc}$ | 1.68 | 1.68 | 1.68 | 1.66 | 1.67 | 1.82 | 1.72 | 1.89 |
| Total | 99.87 | 99.70 | 99.18 | 98.00 | 97.85 | 98.65 | 99.27 | 100.05 |
| **Crystal-chemical formulae recalculated for 25 $O^{2-}$/16 cations** | | | | | | | | |
| Si | 5.905 | 5.843 | 5.834 | 5.895 | 5.909 | 5.946 | 5.854 | 5.990 |
| P | 0.002 | 0.029 | 0.011 | 0.012 | – | 0.017 | – | 0.014 |
| Ti | 0.161 | 0.132 | 0.116 | 0.089 | 0.047 | 0.038 | 0.234 | 0.008 |
| Th | – | 0.017 | 0.022 | 0.046 | 0.019 | 0.006 | 0.001 | – |
| U | 0.003 | – | 0.002 | – | 0.003 | – | – | – |
| Al | 3.372 | 3.671 | 3.752 | 3.793 | 3.862 | 4.353 | 1.842 | 4.425 |
| V | 0.006 | 0.014 | 0.005 | 0.008 | 0.010 | 0.009 | 0.031 | 0.007 |
| Fe | 2.251 | 1.818 | 1.811 | 1.716 | 1.729 | 1.605 | 2.270 | 1.544 |
| Y | 0.001 | 0.003 | 0.002 | 0.003 | 0.012 | 0.005 | – | – |
| La | 0.240 | 0.306 | 0.273 | 0.225 | 0.161 | 0.031 | 0.003 | 0.003 |
| Ce | 0.562 | 0.538 | 0.539 | 0.478 | 0.444 | 0.093 | – | 0.003 |
| Pr | 0.070 | 0.036 | 0.044 | 0.047 | 0.074 | 0.009 | – | – |
| Nd | 0.196 | 0.179 | 0.181 | 0.218 | 0.280 | 0.069 | – | 0.003 |
| Sm | 0.011 | 0.029 | 0.009 | 0.021 | 0.027 | 0.009 | – | 0.003 |
| Gd | 0.013 | 0.004 | 0.011 | 0.008 | 0.020 | 0.001 | 0.009 | 0.001 |
| Mg | 0.130 | 0.287 | 0.268 | 0.238 | 0.232 | 0.034 | 0.010 | 0.009 |
| Ca | 2.610 | 2.722 | 2.765 | 2.849 | 2.814 | 3.608 | 6.545 | 3.941 |
| Mn | 0.033 | 0.038 | 0.046 | 0.038 | 0.047 | 0.045 | 0.032 | 0.034 |
| Na | 0.002 | – | 0.005 | 0.029 | 0.022 | 0.000 | 0.008 | 0.003 |

The leucocratic porphyritic alkali feldspar granites of suite 2 are peraluminous (ASI = 1.09–1.29) with silica content in the narrow range 70–73.8 wt. %, characterized by $K_2O > Na_2O$ as well as high Rb/Sr ratio = 1.97–2.56 and plot in a shoshonitic field (Fig. 3a). They plot as magnesian and ferroan melts (Fig. 3b). The chondrite-normalized REE diagram shows a weak LREE enrichment $(Ce/Yb)_N = 1.94–5.69$ and negative Eu anomaly (Eu/Eu* = 0.419–0.709; Table 4, Fig. 4). The leucogranites show low Zr and Y contents (31.0–19.0 ppm and 6.3–1.5 ppm respectively). Temperatures calculated on the basis of the Zr-geothermometer of Watson & Harrison (1983) for this rock are in the range of 642–682 °C (Table 4).

Comparing both granite suites, the suite 1 granodiorite-tonalite is characterized by higher MgO, $Fe_2O_3$, $TiO_2$, Ba, Zr, Ce, Nd, Sm and Y concentrations then suite 2 leucogranites (Table 4; Fig 5). Granite discrimination diagrams (Pearce et al. 1984) point to a VAG (volcanic arc granites) geotectonic regime of all the analysed rocks (Fig. 6a,b). On a R1-R2 diagram (Batchelor & Bowden 1985) the suite 1 granitoids plot in the pre-plate collision field, while the suite 2 rocks could be classified as late orogenic or anatectic granites (Fig. 3c).

## Results of zircon investigations

### *Suite 1 granitoids (sample G1)*

Zircon crystals are generally clear, colourless, and vary in length from ca. 50 to 250 μm. All zircons are euhedral, differing only in their aspect ratios which range from 1:1 to 1:4 (Fig. 7). The characteristic feature of these crystals is the high content of long-prismatic (length/width ratio >3) zircons (43 %). In most zircons the [110] prism is better developed than [100], with the [211] bipyramid dominating over the [101]. They correspond to subtypes L2–L3 and S2–S3

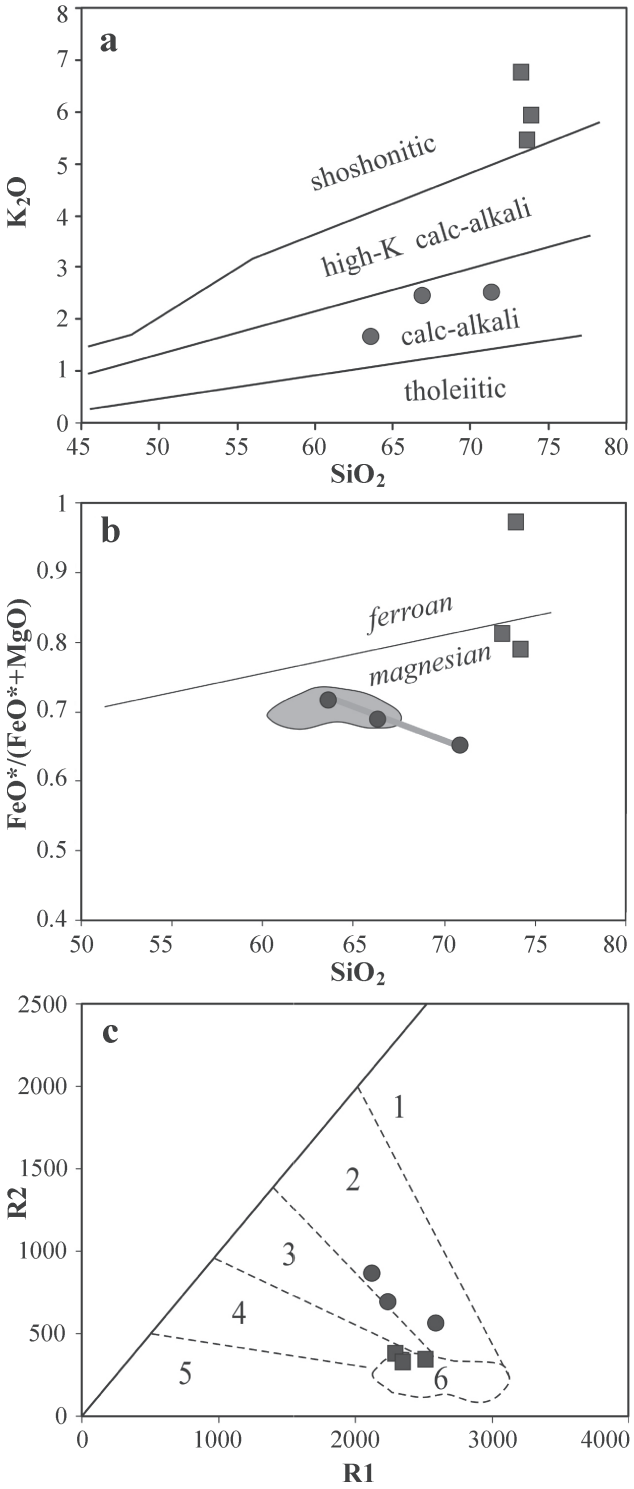


**Fig. 3.** Various plots of the Goryczkowa granites: **a** — plot on $K_2O$ *versus* $SiO_2$ after Pecerillo & Taylor (1976); **b** — plot on FeO*/(FeO*+MgO) *versus* $SiO_2$ after Frost & Frost (2008); **c** — multicationic R1-R2 diagram after de La Roche et al. (1980). Fields are numbered according to Batchelor & Bowden (1985): **1** — mantle fractionates, **2** — pre-plate collision suites, **3** — post-collision suites, **4** — late orogenic magmas, **5** — anorogenic suites, **6** — syn-collisional (anatectic) suites. R1 = 4Si−11(Na+K)−2(Fe+Ti); R2 = 6Ca+2Mg+Al. **Circles** — granitoids from suite 1; **Squares** — granitoids from suite 2.

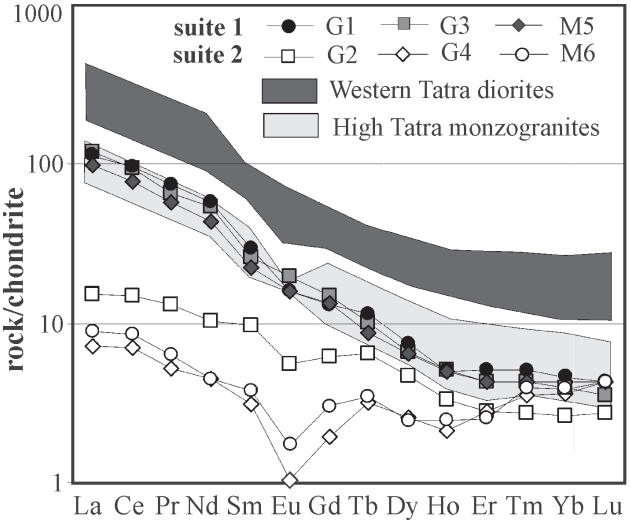


**Fig. 4.** Rare earth elements patterns, normalized to C1 chondrite (after Sun & McDonough 1989), in Goryczkowa granites. The shaded areas show the range of REE patterns of quartz-diorites from the Tatra Mountains (after Gawęda et al. 2005) and High Tatra monzogranites (after Gawęda 2009).

(Fig. 8a; Pupin 1980). CL investigations show that oscillatory zoning is the prominent textural feature, with growth bands varying between fine and broad within individual grains (Fig. 9). Luminescence of growth zoning is variable and mostly moderate. Sporadically, zircons are composed of cores with well-developed oscillatory zoning, indicative of original growth from the melt (Fig. 9; grains: G1_IV_11, G1_III_02, G1_III_15). Some grains have interior domains brighter compared with the external parts. These interior domains have boundaries parallel to external oscillatory zoning (Fig. 9; grains G1_IV_08, G1_III_10) as they are not considered to be inherited cores. The external domains occur mainly as euhedral pyramidal tips with oscillatory zoning, which appear dark under CL (corresponding to relatively high U contents and higher degrees of metamictization, Fig. 9).

Twenty two LA-MC-ICP-MS U-Pb measurements on fourteen crystals were made (Fig. 9; Table 5). All data points are concordant within the assigned error (Fig. 10). Sixteen analyses from the oscillatory-zoned zircon yield a concordia age of 371±6.0 Ma (MSWD = 1.6, Fig. 10a, group A). Four inherited cores plot as 433±21 Ma (MSWD = 3.1, Fig. 10b, group B) and two other give an age of ca. 2650 Ma and 2530 Ma (Table 5).

### *Suite 2 granitoids (sample G2)*

The zircons are euhedral, mainly normal-prismatic crystals with aspect ratio 1:2 to 1:6. Grain size varies in length from ca. 50 to 250 μm (Fig. 11). Zircons appear clear, colourless to pink. In most crystals [110] prisms are better developed than [100] and the [211] bipyramid dominates over the [101], what make them very similar to the population of the suite 1 (Figs. 8a,b). The main difference from the suite 1 is that some of crystals show larger [100] prisms and [211] pyramids. These features correspond to subtypes J2

| | Suite 1 | | | Suite 2 | | |
|---|---|---|---|---|---|---|
| **Sample No.** | **G1** | **G3** | **M5** | **G2** | **G4** | **M6** |
| $SiO_2$ | 66.34 | 63.61 | 70.87 | 73.94 | 73.1 | 73.87 |
| $TiO_2$ | 0.56 | 0.75 | 0.29 | 0.06 | 0.03 | 0.02 |
| $Al_2O_3$ | 16.82 | 17.47 | 15.53 | 14.62 | 15.06 | 13.91 |
| $Fe_2O_{3T}$ | 3.65 | 4.48 | 2.25 | 0.78 | 0.42 | 0.46 |
| MnO | 0.06 | 0.07 | 0.04 | 0.02 | 0.005 | 0.08 |
| MgO | 1.48 | 1.59 | 1.08 | 0.18 | 0.09 | 0.00 |
| CaO | 2.71 | 4.03 | 1.67 | 0.41 | 0.58 | 0.44 |
| $Na_2O$ | 4.26 | 4.52 | 4.17 | 2.86 | 2.89 | 3.81 |
| $K_2O$ | 2.46 | 1.55 | 2.52 | 5.91 | 6.68 | 5.46 |
| $P_2O_5$ | 0.21 | 0.29 | 0.12 | 0.21 | 0.13 | 0.09 |
| LOI | 1.30 | 1.40 | 1.20 | 1.00 | 1.00 | 0.68 |
| **Total** | **99.85** | **99.76** | **99.74** | **99.99** | **99.985** | **98.82** |
| Sr | 632.8 | 838.2 | 603.2 | 81.3 | 79.8 | 42.0 |
| Ba | 780.9 | 550 | 1234 | 418.9 | 179 | 213.0 |
| Rb | 78.9 | 41.3 | 52.3 | 208.9 | 157.5 | 90.0 |
| Th | 10.2 | 11.2 | 7.0 | 3.5 | 1.6 | 0.54 |
| U | 1.8 | 1.3 | 1.3 | 1.1 | 2.8 | 0.63 |
| Ga | 20.5 | 18.5 | 17.3 | 20.6 | 14.6 | 12.0 |
| Ni | 7.1 | 5.3 | 5.5 | 2.6 | 1.1 | 9.0 |
| Cr | 75 | 130 | 13.7 | 89 | 48 | 33 |
| Zr | 171 | 155.7 | 124 | 31 | 25.2 | 19 |
| Hf | 4.8 | 4.3 | 3.4 | 1.4 | 1.5 | 1.0 |
| Y | 9.8 | 7.3 | 8.3 | 6.3 | 4.6 | 1.5 |
| Nb | 7.4 | 5.4 | 3.5 | 10.5 | 10.5 | 1.3 |
| Ta | 0.6 | 0.2 | 0.3 | 1.4 | 5.1 | 1.2 |
| La | 26.3 | 28.6 | 23.6 | 3.6 | 1.7 | 2.1 |
| Ce | 58.9 | 58.8 | 48 | 9.3 | 4.3 | 5.3 |
| Pr | 7.04 | 6.23 | 5.51 | 1.26 | 0.5 | 0.6 |
| Nd | 27 | 25.2 | 20.5 | 4.8 | 2.1 | 2.11 |
| Sm | 4.5 | 4.03 | 3.44 | 1.5 | 0.48 | 0.58 |
| Eu | 0.93 | 1.15 | 0.92 | 0.32 | 0.06 | 0.1 |
| Gd | 2.68 | 3.05 | 2.77 | 1.27 | 0.4 | 0.63 |
| Tb | 0.43 | 0.38 | 0.33 | 0.24 | 0.12 | 0.13 |
| Dy | 1.91 | 1.67 | 1.65 | 1.18 | 0.65 | 0.63 |
| Ho | 0.28 | 0.29 | 0.28 | 0.19 | 0.12 | 0.14 |
| Er | 0.85 | 0.71 | 0.71 | 0.46 | 0.46 | 0.42 |
| Tm | 0.13 | 0.11 | 0.11 | 0.07 | 0.09 | 0.1 |
| Yb | 0.78 | 0.67 | 0.73 | 0.45 | 0.61 | 0.65 |
| Lu | 0.11 | 0.09 | 0.11 | 0.07 | 0.11 | 0.11 |
| **ASI** | **1.193** | **1.109** | **1.259** | **1.289** | **1.183** | **1.090** |
| $Na_2O/K_2O$ | 1.732 | 2.916 | 1.655 | 0.484 | 0.433 | 0.698 |
| Rb/Sr | 0.125 | 0.049 | 0.087 | 2.569 | 1.974 | 2.143 |
| Nd/Th | 2.647 | 2.250 | 2.929 | 1.371 | 1.313 | 3.907 |
| ΣREE | 131.84 | 130.98 | 108.66 | 24.71 | 11.7 | 13.6 |
| Eu/Eu* | 0.819 | 1.003 | 0.911 | 0.709 | 0.419 | 0.506 |
| $Ce_N/Yb_N$ | 20.806 | 24.181 | 18.117 | 5.694 | 1.942 | 2.247 |
| $T_{Zr}$ [°C] | 793 | 768 | 780 | 682 | 663 | 643 |

**Table 4:** Chemical composition and selected petrological indicators of granitoid rocks from the crystalline cores, Tatra Mountains. Major element and trace element concentrations in wt. % and ppm, respectively. Explanations: **G** — Goryczkowa crystalline core; **M** — Małołączniak crystalline core; **LOI** — lost of ignition; **Eu/Eu*** = Eu/(√Sm·Gd); **ASI**=$Al_2O_3/(CaO+Na_2O+K_2O-3.33\ P_2O_5)$ in molecular units.

(Fig. 12, crystal G2_III_02) and S22 (Pupin 1980). Most grains are characterized by well-developed oscillatory zoning, ranging from fine to broad and display variable luminescence. The majority of grains lack discernible, inherited cores, but where preserved, cores are rounded, zoned and distinct from enclosing rims by virtue of luminescence and truncated zoning (Fig. 12; grains G2_IIb_15, G2_III_12). These features suggest that the internal domains are detrital zircon cores that underwent physical abrasion before the formation of the overgrowth. The cores sometimes make up about 80–90 % of the grains by volume, although most frequently the overgrowths predominate. The cores show well-developed oscillatory zoning indicating an igneous (felsic) source. The boundary between core and overgrowth is marked by an irregular light band (Fig. 12; grains G2_IIb_15, G2_III_12).

Seventeen LA-MC-ICP-MS U-Pb measurements on thirteen crystals were made (Fig. 12; Table 6). All data points are concordant within the assigned error. Twelve spot analyses span a range in dates from 387 to 350 Ma, with five inherited cores giving substantially older dates of ca. 1780 Ma and 420 Ma (Fig. 12; Table 6). Nine analyses from the oscillatory-zoned zircon (subtype L2-S3) yield a concordia age of 350 ± 4.7 Ma (MSWD = 0.68; Figs. 12, 13; Table 6 — group A) while three analyses from the oscillatory-zoned zircon (subtype J2-S22) yield a concordia age of 387 ± 11 Ma (MSWD = 2.9; Figs. 12, 13; Table 6 — group B). Two inherited cores yield an age of 412 ± 9 Ma (MSWD = 3; Fig. 12; Table 6 — group C), two others are discordant and one yields a concordant age of ca. 1773 ± 55 (Fig. 12; Table 6 — groups D and E).

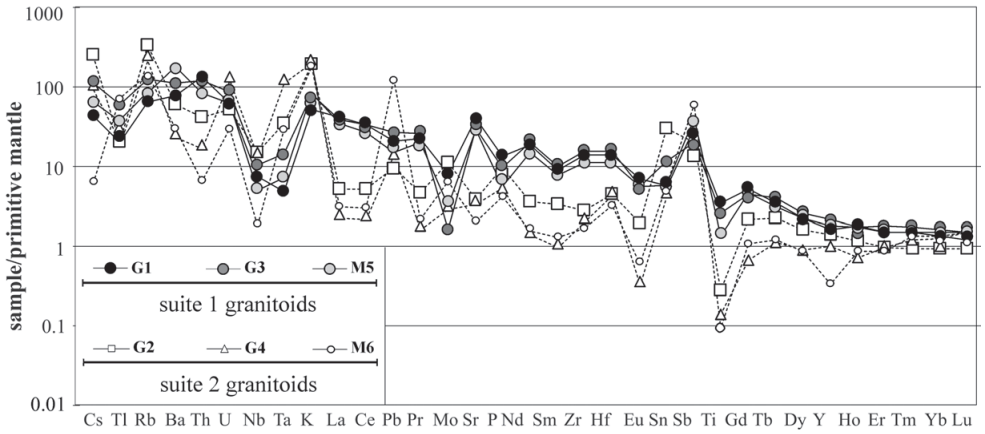


**Fig. 5.** Primitive mantle normalized (after Sun & McDonough 1989) trace element diagram of analysed granitoids. **G** — Goryczkowa crystalline core; **M** — Małołączniak crystalline core.

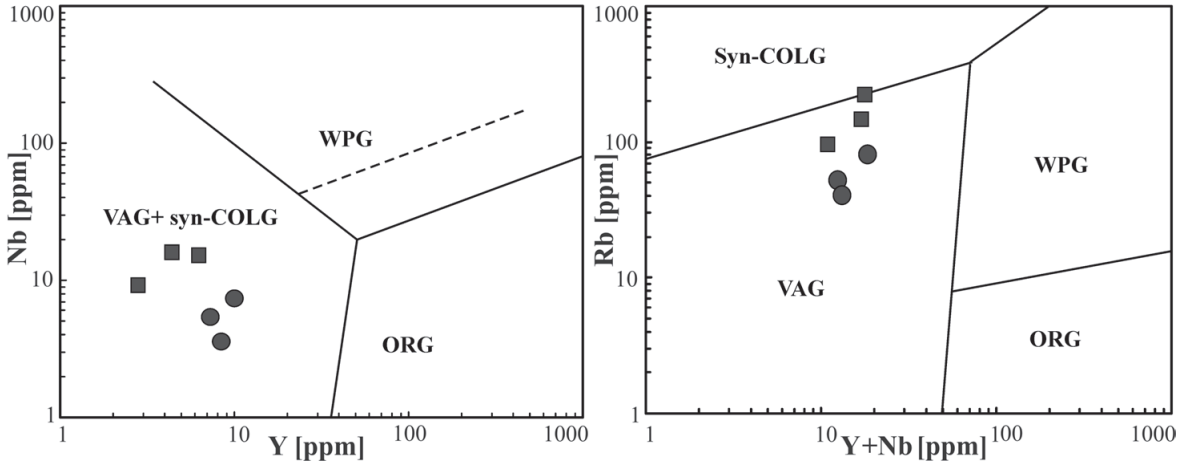


**Fig. 6.** Plot of the Goryczkowa granites in the Pearce et al. (1984) discrimination diagrams. Abbreviations: **VAG** — volcanic arc granites, **syn-COLG** — syn-collisional granites, **WPG** — within-plate granites, **ORG** — ocean ridge granites. **Circles** — granitoids from suite 1; **Squares** — granitoids from suite 2.

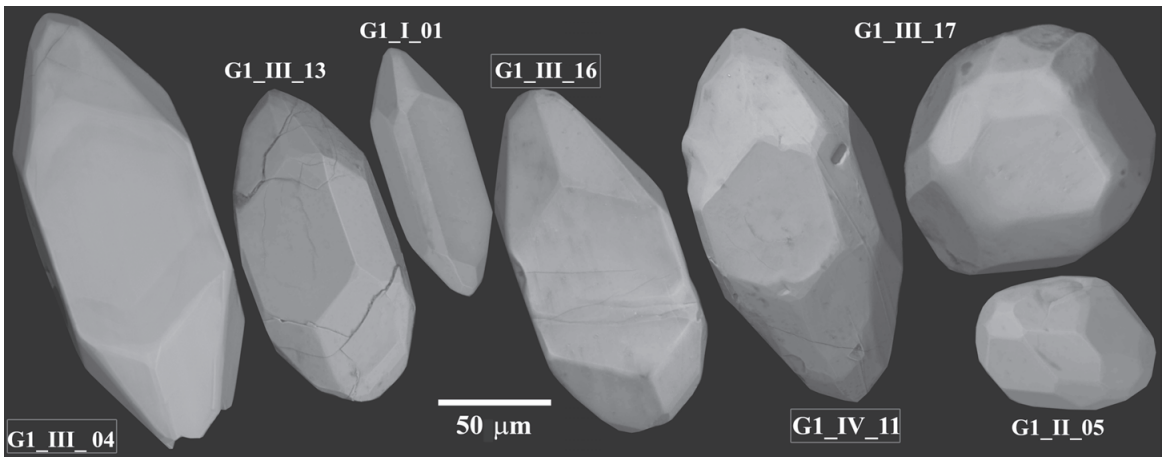


**Fig. 7.** Secondary electron (SEM) images of selected zircon crystals from granodiorite (sample G1— suite 1). Zircon crystals with numbers in frames are also imaged by CL in Figure 9. See text for description.

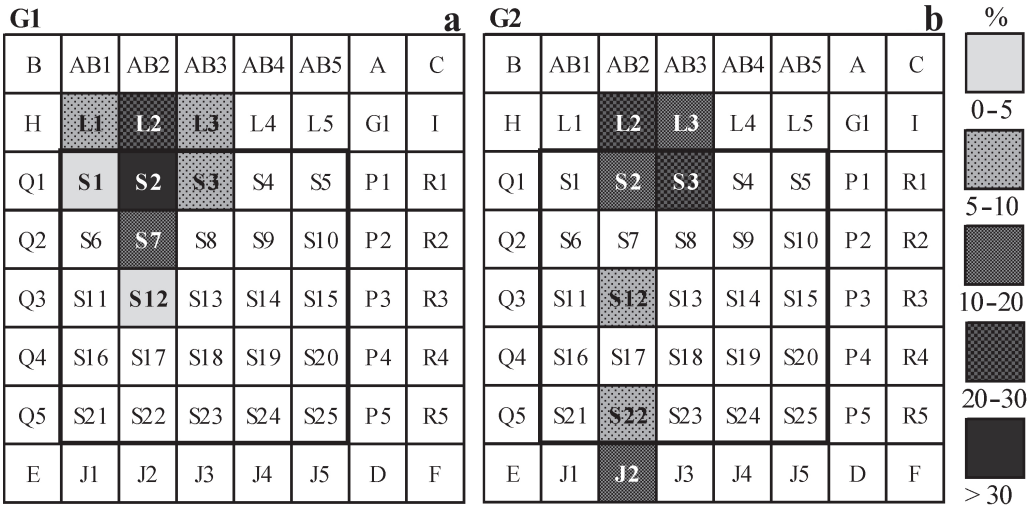


**Fig. 8.** Typological frequency distribution of euhedral zircon crystals from (**a**) granodiorite, sample G1, suite 1, and from (**b**) leucogranite, sample G2, suite 2 (according to the classification of Pupin 1980).

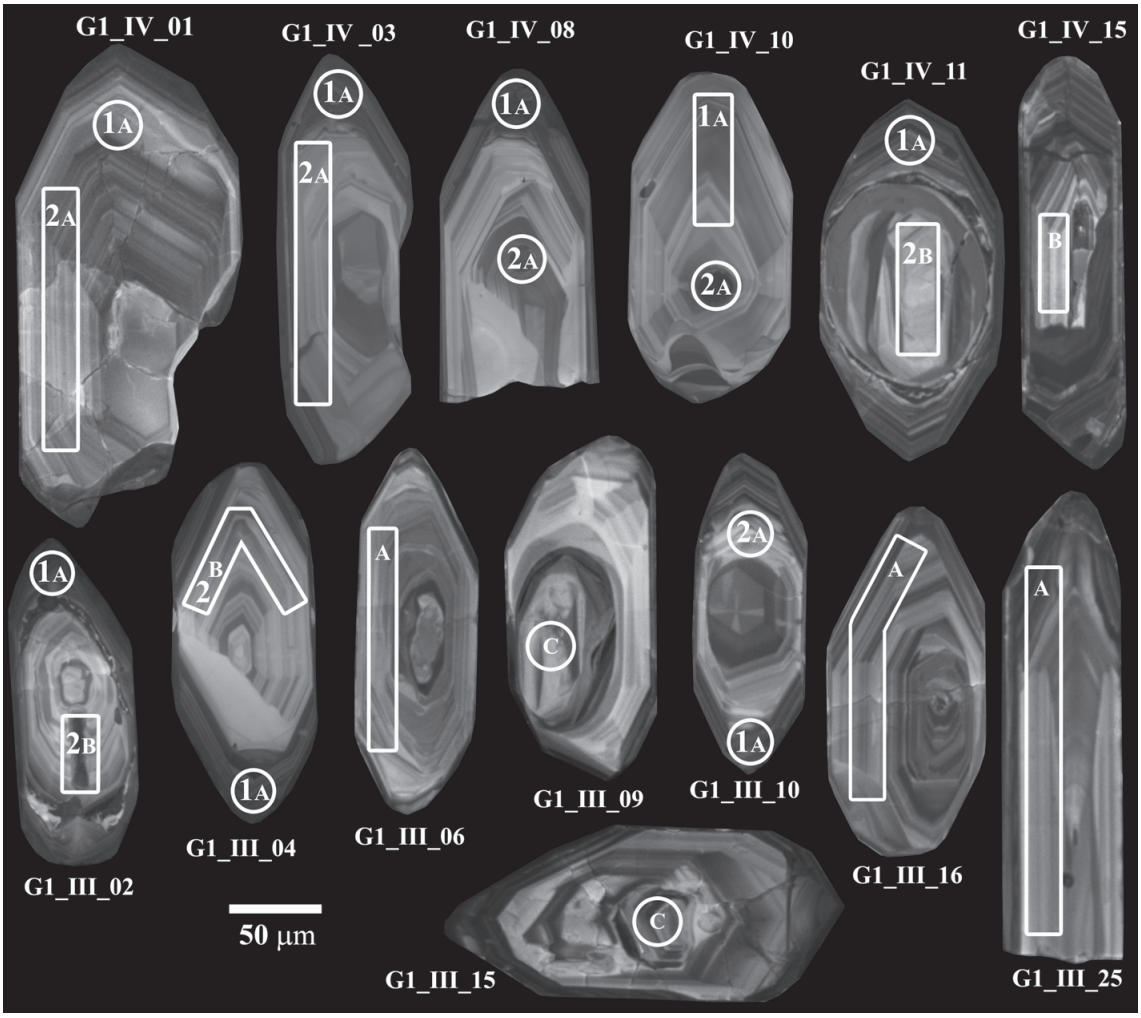


**Fig. 9.** Compiled cathodoluminescence (CL) images showing the range of textures observed in zircon crystals from granodiorite (sample G1 — suite 1). See text for details. The white rectangles and circles show the approximate location of laser ablation trenches (confirmed by re-inspecting grains under cathodoluminescence after the dating session) and are not to scale. The numbers refer to the analytical data presented in Table 5.

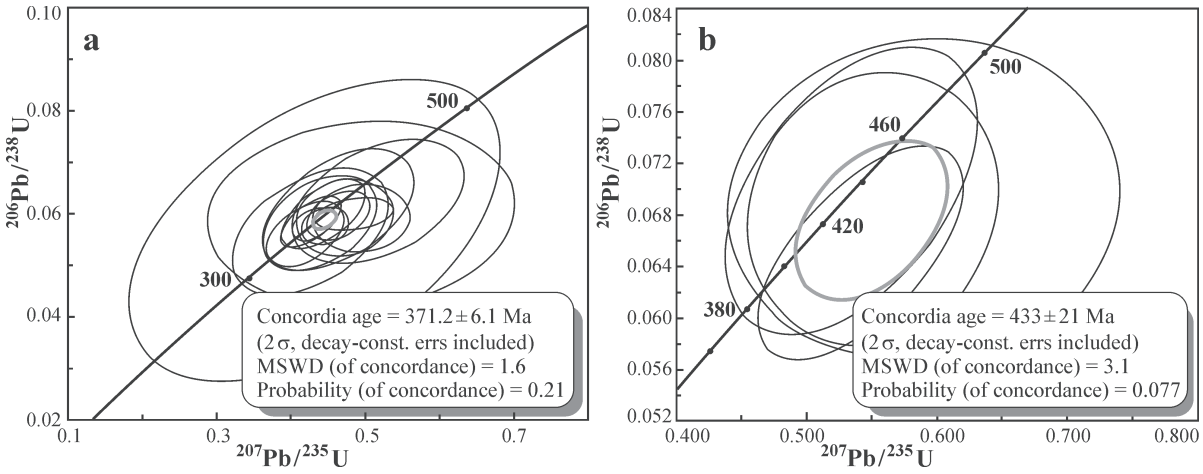


**Fig. 10.** Concordia plots of LA-MC-ICP-MS U-Pb zircon analytical results from granodiorite (sample G1 — suite 1). Open error ellipses are isotope ratios of individual grain spots: **a** — the main group of analyses (n=11) of oscillatory zoned zircons; **b** — inherited cores (xenocrysts) with oscillatory, magmatic zoning. Inherited cores at ca. 2560 Ma not shown on diagram. Thick error ellipse corresponds to the 2 σ and 95% confidence errors of the calculated concordia ages.

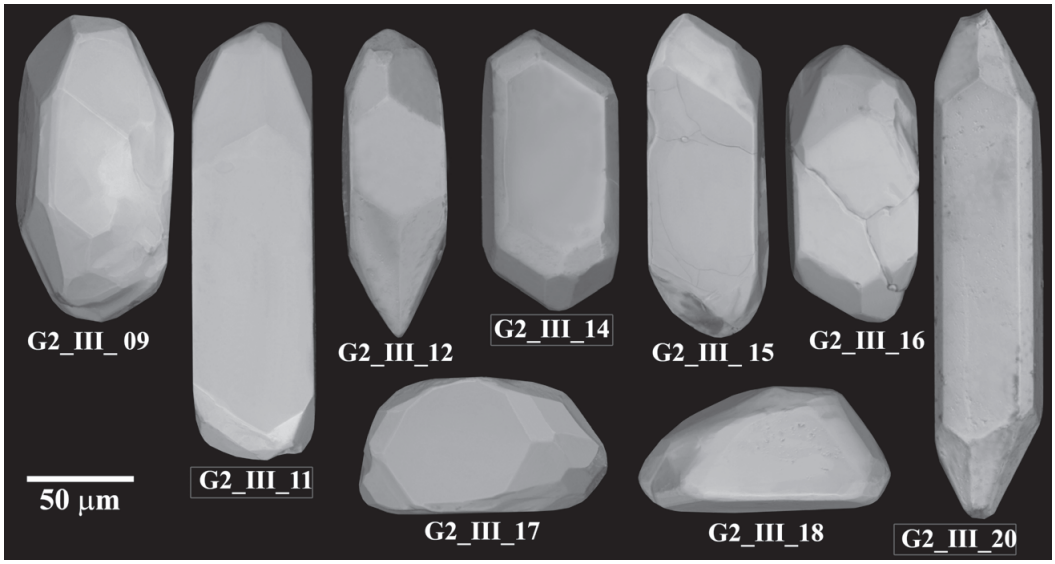


**Fig. 11.** Secondary electron (SEM) images of selected zircon crystals from leucogranite (sample G2 — suite 2). Zircon crystals with numbers in frame are also imaged by CL in Figure 12. See text for description.

**Table 5:** LA-MC-ICP-MS U-Pb zircon data from granodiorite (sample G1 — suite 1). Explanations: ***** — final blank corrected intensities in μV; **#** — final blank corrected intensities in mV; **2SD** — the 2 sigma standard deviation (in percent); **Rho** — error-correlation between the $^{206}Pb/^{238}U$ and $^{207}Pb/^{235}U$ ratios.

| Group | File name | Final blank corrected intensities | | | | Final mass bias and common Pb corrected ratios | | | | | | | Concordia age (Ma) |
|---|---|---|---|---|---|---|---|---|---|---|---|---|---|
| | | $^{204}Pb^{*}$ | $^{206}Pb^{\#}$ | $^{207}Pb^{\#}$ | $^{238}U^{\#}$ | $^{207}Pb/^{206}Pb$ | 2SD (%) | $^{207}Pb/^{235}U$ | 2SD (%) | $^{206}Pb/^{238}U$ | 2SD (%) | Rho | |
| A | G1_IV_01/1 | 2.495 | 0.383 | 0.031 | 16.76 | 0.0550 | 9.2 | 0.4641 | 17.7 | 0.0608 | 15.7 | 0.48 | **371 ± 6.0** |
| | G1_IV_01/2 | 1.896 | 1.359 | 0.085 | 39.45 | 0.0580 | 4.8 | 0.4723 | 11.3 | 0.0593 | 10.2 | 0.13 | |
| | G1_IV_03/1 | 0.895 | 0.562 | 0.046 | 25.34 | 0.0530 | 5.4 | 0.4187 | 10.4 | 0.0561 | 9.2 | 0.49 | |
| | G1_IV_03/2 | 2.561 | 1.777 | 0.105 | 52.16 | 0.0560 | 3.0 | 0.4459 | 5.8 | 0.0576 | 5.1 | 0.19 | |
| | G1_IV_08/1 | 1.069 | 0.263 | 0.024 | 11.77 | 0.0616 | 2.5 | 0.4848 | 8.9 | 0.0599 | 4.3 | 0.27 | |
| | G1_IV_08/2 | 7.209 | 1.407 | 0.101 | 47.16 | 0.0695 | 15.6 | 0.4949 | 34.3 | 0.0599 | 24.6 | 0.10 | |
| | G1_IV_10/1 | 0.607 | 0.692 | 0.056 | 30.03 | 0.0532 | 5.4 | 0.4440 | 10.4 | 0.0600 | 9.2 | 0.59 | |
| | G1_IV_10/2 | 0.730 | 0.122 | 0.011 | 5.37 | 0.0564 | 3.7 | 0.4640 | 7.4 | 0.0597 | 6.4 | 0.37 | |
| | G1_IV_11/1 | 1.138 | 0.208 | 0.019 | 10.53 | 0.0599 | 10.2 | 0.4261 | 20.2 | 0.0565 | 17.7 | 0.45 | |
| | G1_III_02/1 | 2.015 | 0.261 | 0.024 | 11.51 | 0.0577 | 2.7 | 0.4285 | 5.2 | 0.0580 | 4.6 | 0.41 | |
| | G1_III_04/1 | 1.964 | 2.413 | 0.138 | 75.30 | 0.0561 | 7.4 | 0.4388 | 14.4 | 0.0583 | 12.7 | 0.38 | |
| | G1_III_06 | 2.452 | 4.183 | 0.252 | 123.85 | 0.0549 | 14.9 | 0.4445 | 28.9 | 0.0584 | 25.5 | 0.21 | |
| | G1_III_10/1 | 1.369 | 1.236 | 0.072 | 36.64 | 0.0564 | 24.4 | 0.4325 | 47.4 | 0.0569 | 41.9 | 0.50 | |
| | G1_III_10/2 | 1.858 | 0.610 | 0.039 | 19.66 | 0.0643 | 5.5 | 0.4948 | 10.8 | 0.0591 | 9.1 | 0.06 | |
| | G1_III_16 | 1.434 | 1.423 | 0.089 | 41.75 | 0.0591 | 9.0 | 0.5174 | 18.3 | 0.0624 | 15.9 | 0.41 | |
| | G1_III_25 | 0.701 | 0.386 | 0.032 | 17.68 | 0.0568 | 4.0 | 0.4266 | 7.8 | 0.0585 | 6.9 | 0.65 | |
| B | G1_IV_11/2 | 0.980 | 0.816 | 0.051 | 22.07 | 0.0619 | 6.1 | 0.5416 | 11.8 | 0.0650 | 10.4 | 0.63 | **433 ± 21** |
| | G1_IV_15 | 2.754 | 0.326 | 0.028 | 9.58 | 0.0715 | 73.4 | 0.5508 | 14.2 | 0.0685 | 12.6 | 0.11 | |
| | G1_III_02/2 | 0.586 | 0.281 | 0.024 | 10.47 | 0.0557 | 7.6 | 0.5341 | 14.8 | 0.0699 | 13.0 | 0.49 | |
| | G1_III_04/2 | 2.306 | 0.299 | 0.027 | 8.75 | 0.0765 | 9.8 | 0.5903 | 20.8 | 0.0690 | 15.0 | 0.06 | |
| C | G1_III_09 | 4.966 | 14.01 | 2.591 | 53.22 | 0.1705 | 2.6 | 11.057 | 5.0 | 0.4690 | 4.4 | 0.54 | **2529 ± 47** |
| | G1_III_15 | 3.663 | 15.21 | 2.976 | 50.71 | 0.1801 | 3.9 | 12.595 | 8.1 | 0.4990 | 7.1 | 0.44 | **2648 ± 76** |

## Discussion

### *Ages of granitoids*

The zircon LA-MC-ICP-MS U-Pb data from suite 1 provide the first constraint on the crystallization ages of the Goryczkowa type granitoids at ca. 371 ± 6.0 (Fig. 10a; Table 5). This age is older than the Rb-Sr isochron age of 300 Ma given by Burchart (1968, 1970) and comparable with the upper limit of granitoid magmatism in the Goryczkowa Unit (ca. 370 Ma) suggested by Kohút & Siman (2011). The Late Devonian age was also obtained from a tonalite in the Branisko Mts (Kohút et al. 2010), from hybrid granitoids in the Western Tatra Mts (Burda et al. 2011) and from an enclave-bearing tonalite and associated dykes of the Tribeč Mts (Broska et al. 2013).

Zircon crystals from suite 2 (sample G2) are characterized by oscillatory zoning with intermittent dissolution surfaces (Fig. 12) representing corrosion or resorption events during evolution of a zircon crystal (e.g. Vavra 1990,

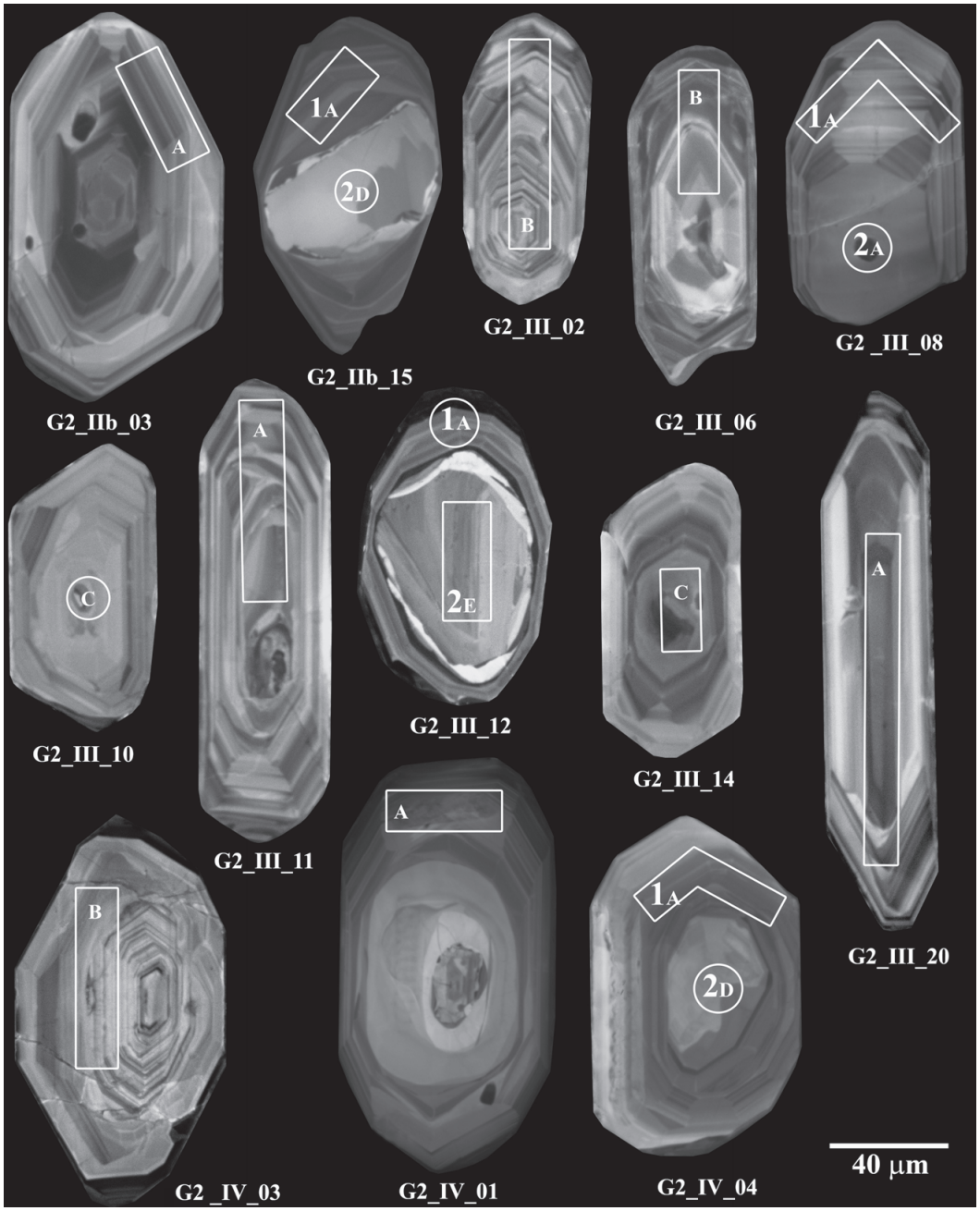


**Fig. 12.** Cathodoluminescence (CL) images of selected zircon crystals from leucogranite (sample G2). All grains have a prismatic habitus characteristic for a magmatic origin. See text for description. The white rectangles and circles show the approximate location of laser ablation trenches and are not to scale. The numbers refer to the analytical data presented in Table 6.

1994). These crystals belong to two typological groups on the Pupin's (1980) diagram (Fig. 8b). The first typology group (L2–L3 to S2–S3 subtypes) with intermittent dissolution surfaces, plots in the upper part of the diagram and yields a concordia age of 350±5 Ma (Figs. 8b, 13a). The second group plots in the lower part of the typology diagram (S22 and J2 subtypes) and yields an age of 387±11 Ma (Figs. 8b, 13b).

In both suites inherited cores giving substantially older dates of 433±21 Ma (suite 1; Table 5) and 412±9 Ma (suite 2; Table 6) indicate the presence of a magmatic component in the melted source. These ages are in agreements with the whole-rock Rb-Sr dating (413 Ma) and support the early thesis about the Early Silurian age of the thermal event in the Tatra Mountains (Burchart 1968, 1970). Similar ages from oscillatory zoned zircon cores, indicating Caledonian (450–460 Ma) magmatism, found recently in the High Tatra Mts (Burda et al. 2013), are in accordance with findings of Late Ordovician-Early Silurian magmatic episodes in the Veporic crystalline complex (ca. 470 Ma; Janák et al. 2002; Gaab et al. 2003) and Tatric crystalline basement (450 and 430 Ma; Kohút et al. 2008; Putiš et al. 2009).

**Table 6:** LA-MC-ICP-MS U-Pb zircon data from leucogranite (sample G2 — suite 2). Explanations: * — final blank corrected intensities in μV; # — final blank corrected intensities in mV; **2SD** — the 2 sigma standard deviation (in percent); **Rho** — error-correlation between the $^{206}Pb/^{238}U$ and $^{207}Pb/^{235}U$ ratios.

| Group | File name | Final blank corrected intensities (in V) | | | | Final mass bias and common Pb corrected ratios | | | | | | | Concordia age (Ma) |
|---|---|---|---|---|---|---|---|---|---|---|---|---|---|
| | | $^{204}Pb^*$ | $^{206}Pb^\#$ | $^{207}Pb^\#$ | $^{238}U^\#$ | $^{207}Pb/^{206}Pb$ | 2SD (%) | $^{207}Pb/^{235}U$ | 2SD (%) | $^{206}Pb/^{238}U$ | 2SD (%) | Rho | |
| A | G2_IIb_03 | 0.984 | 0.413 | 0.017 | 9.97 | 0.0540 | 1.6 | 0.4101 | 3.0 | 0.0550 | 2.7 | 0.44 | **350 ± 4.7** |
| | G2_IIb_15/1 | 1.271 | 1.741 | 0.106 | 62.37 | 0.0544 | 4.6 | 0.4103 | 9.0 | 0.0552 | 7.9 | 0.32 | |
| | G2_III_08/1 | 1.110 | 0.413 | 0.017 | 10.40 | 0.0545 | 2.8 | 0.4112 | 5.4 | 0.0545 | 4.8 | 0.17 | |
| | G2_III_08/2 | 0.902 | 0.500 | 0.041 | 22.26 | 0.0558 | 3.3 | 0.4285 | 6.5 | 0.0566 | 5.7 | 0.30 | |
| | G2_III_11 | 0.981 | 0.526 | 0.041 | 22.88 | 0.0534 | 3.7 | 0.4129 | 7.1 | 0.0557 | 6.3 | 0.52 | |
| | G2_III_12/1 | 0.675 | 0.304 | 0.013 | 7.43 | 0.0525 | 3.9 | 0.4154 | 7.6 | 0.0575 | 6.7 | 0.29 | |
| | G2_III_20 | 1.398 | 0.413 | 0.017 | 9.80 | 0.0539 | 3.2 | 0.4171 | 6.2 | 0.0567 | 5.5 | 0.43 | |
| | G2_IV_01 | 1.206 | 0.208 | 0.017 | 9.21 | 0.0574 | 3.4 | 0.4231 | 6.6 | 0.0561 | 5.8 | 0.38 | |
| | G2_IV_04/1 | 0.755 | 0.704 | 0.039 | 23.77 | 0.0527 | 4.1 | 0.4016 | 8.0 | 0.0563 | 7.0 | 0.27 | |
| B | G2_III_02 | 1.126 | 1.242 | 0.076 | 36.11 | 0.0552 | 9.4 | 0.4564 | 11.1 | 0.0618 | 9.0 | 0.30 | **387 ± 11** |
| | G2_III_06 | 0.941 | 0.236 | 0.021 | 10.38 | 0.0616 | 2.4 | 0.4790 | 4.7 | 0.0612 | 4.1 | 0.35 | |
| | G2_IV_03 | 1.662 | 0.841 | 0.060 | 28.00 | 0.0604 | 5.0 | 0.4667 | 10.0 | 0.0590 | 8.6 | 0.27 | |
| C | G2_III_10 | 1.356 | 0.234 | 0.021 | 9.65 | 0.0617 | 3.0 | 0.5185 | 5.8 | 0.0646 | 5.1 | 0.24 | **412 ± 9** |
| | G2_III_14 | 1.096 | 0.763 | 0.061 | 28.88 | 0.0551 | 1.8 | 0.5048 | 3.5 | 0.0653 | 3.1 | 0.41 | |
| D | G2_IIb_15/2 | 4.029 | 0.705 | 0.068 | 17.17 | 0.0897 | 11.3 | 0.8751 | 22.0 | 0.0679 | 19.5 | 0.51 | **disc.** |
| | G2_IV_04/2 | 10.697 | 1.708 | 0.185 | 55.88 | 0.1106 | 22.3 | 0.8626 | 44.6 | 0.0567 | 37.1 | 0.08 | |
| E | G2_III_12/2 | 3.003 | 7.271 | 0.875 | 42.41 | 0.1110 | 3.4 | 4.7313 | 6.6 | 0.3185 | 5.8 | 0.57 | **1773 ± 55** |

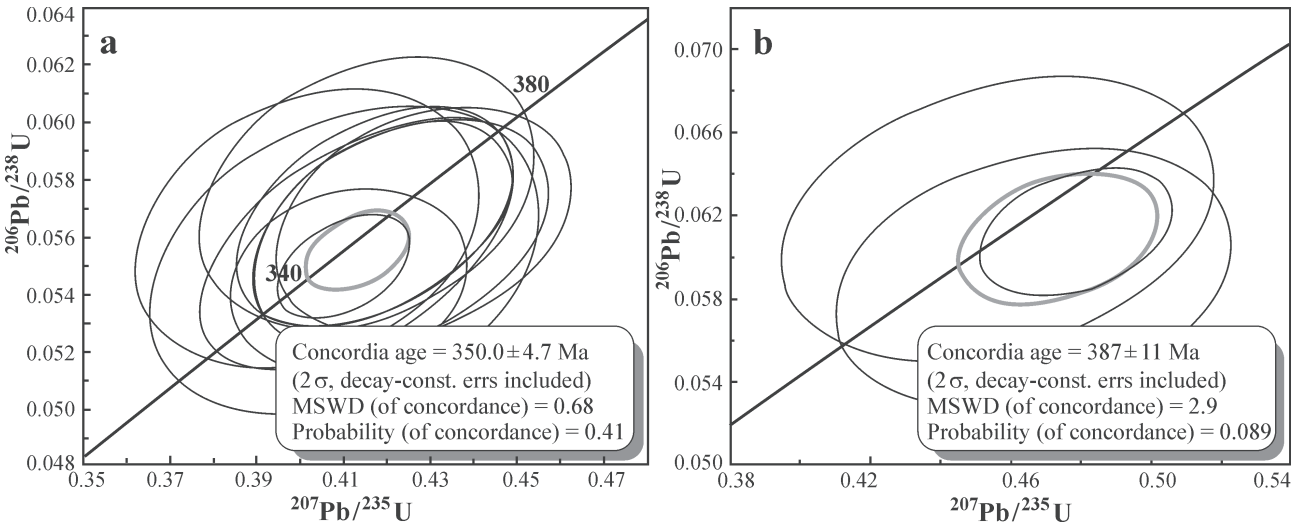


**Fig. 13.** Concordia plots of LA-MC-ICP-MS U-Pb zircon analytical results from leucogranite (sample G2 — suite 2). Open error ellipses are isotope ratios of individual grain spots: **a** — the main group of analyses (n = 9) of oscillatory zoned zircons (zircon L2–S3) with moderate luminescence; **b** — xenocrysts (zircons J2–S22) with oscillatory, magmatic zoning. Inherited cores at ca. 1780 Ma and 420 Ma not shown on the diagram. Thick error ellipse corresponds to the 2σ and 95% confidence errors of the calculated concordia ages.

That allow us to suggest possible connections to the Rebra-Tulghes Terrane (Inner Eastern Carpathians), which docked to the SW margin of Baltica (Balintoni et al. 2009) and the 470–460 Ma magmatic episode in the Somes Terrane of the Southern Carpathians (Apuseni Mountains; Balintoni et al. 2010) and consequently shows the intense, collision-related, tectono-magmatic event. The presence of "Caledonian" magmatic zircons also poses a question about the plate dynamics in the Circum-Carpathians area in the Early Paleozoic and participation of the Avalonian-Cadomian crust in the Variscan tectono-thermal episodes (see discussion in: Gawęda & Golonka 2011).

### *Problem of source rocks and tectonic setting of the granitoid magma*

Major elements chemistry, as proved by Patiño Douce (1999), can indicate the character of melted material. Melts derived from amphibolites and mafic pelites have lower alkali and aluminium contents, but are enriched in calcium, titanium, iron and magnesium. Suite 1 granitoids are, however, peraluminous, which is typical of melted felsic sources. Suite 1 granitoids plot in the field of melts generated from amphibolite–pelite sources (calc-alkali I-type granites; Patiño Douce 1999; Fig. 14).

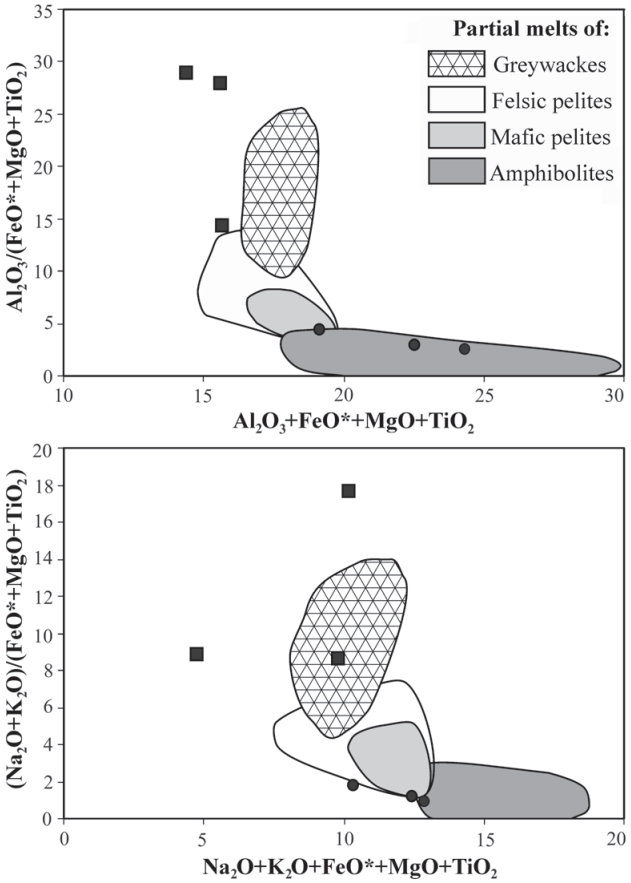


**Fig. 14.** Chemical composition of Goryczkowa granitoids in major oxide diagrams after Patiño Douce (1999). Outlined fields denote compositional fields of experimental melts derived from partial melting of felsic pelites, metagreywackes and amphibolites. **Circles** — granitoids from suite 1; **Squares** — granitoids from suite 2.

Computed oxygen fugacity, expressed as $\log fO_2$, falls in the narrow range from –10.4 to –11.7, and the computed water content in the melt was at 7.8–8.1 wt. % (Ridolfi et al. 2010; Table 2). The oxygen fugacity is higher in relation to values computed for I-type granites from the Inner Carpathians and High Tatra Mountains (compare: Gawęda 2009; Broska & Petrík 2011). Calculations of the accessible published data point out that the relatively similar oxygen fugacities ($\log fO_2$ in the range of –12 to –13) could be found in the hybrid quartz-diorites and associated granitoids from the Western Tatra Mountains (Burda et al. 2011). High oxygen fugacity in suite 1 could be interpreted as the primary magmatic feature, as high-Ca plagioclase is preserved ($An_{45-62}$), so magmatic deanorthitization process, proposed by Broska & Petrík (2011) was observed only sporadically. Pressure–temperature calibrations, based on amphibole and plagioclase compositions, indicated 5.8–6.3 kbar (Schmidt 1992) and 780–810 °C (Blundy & Holland 1990), which agree with Zr-geothermometry (Table 4). The calculations are consistent with the presence of magmatically zoned allanite-epidote, which is stable in dioritic-tonalitic magmas in pressures above 6 kbars with water content near 9 wt. % and oxygen fugacity above QMF (Quartz-Magnetite-Fayalite) buffer (Schmidt & Poli 2004).

This all suggests at least lower crustal/upper mantle provenance of the melt parental for the suite 1 granitoids. Such contradictory features and source rocks interpretations are typical of magmas resulting from mixing/mingling of different magmas (compare Burda et al. 2011) and these complex processes could be suggested for the suite 1 granitoids.

In contradiction, suite 2 granitoids show simple mineral composition as well as enrichment in alkali and alumina, typical of muscovite-dehydration partial melting of felsic pelites (Patiño Douce 1999; Fig. 14), which is consistent with simple mineral composition and peraluminous character (Table 4), while rock-textures suggest disequilibrium at the early stages of crystallization (Fig. 2c).

The contrasting features of both granitoid suites are in agreement with their geotectonic positions on R1-R2 diagram (Fig. 3c).

Trace elements also support the difference between granitoids: suite 1 shows low Rb/Sr and high Nd/Th ratios, typical of lower crustal or mantle-related melts, while high Rb/Sr, together with lower Nd/Th point out upper crustal, highly fractionated character of the suite 2 granitoids. The higher LREE content in suite 1 (Fig. 5) and consequently higher REE fractionation (Fig. 4; Table 4) is a consequence of the allanite-epidote presence (Table 3), sporadically associated with monazite, governing the REE budget in oxidized magmas. Primitive mantle-normalized $[Th/U]_N$ ratios in suite 1 granitoids are relatively high (1.3–2.13), while positive U anomaly $[Th/U]_N$ ratios in the range of 0.14–0.78 is typical of suite 2 granitoids (Fig. 5). As uranium is usually mobilized in highly oxidized melts, the predominace of Th over U in suite 1 granitoids might reflect a contribution from relatively Th-enriched mantle and/or crustal fluids during melting (Kemp & Hawkesworth 2005), supported by the predominance of Th over U in magmatic epidote (Table 3). However, the common presence of secondary muscovite, influencing the ASI value, might also cause the mobilization of some elements.

Both granitoids show VAG affinity (Fig. 6a,b) which is typical of Central European granitoid magmatism (Finger et al. 1997; Gawęda & Golonka 2011). In primitive mantle-normalized multi-element diagrams (Sun & McDonough 1989) negative Nb and Ta anomalies in suite 1 granitoids are more prominent, suggesting typical arc setting (Thirwall et al. 1994), while granitoids of suite 2 show only Nb negative anomaly while Ta is enriched (Fig. 5), suggesting another process (fractional crystallization?), overlapping the typical source characteristic.

### *The problem of zircon inheritance*

The distributions of inherited zircon cores in both rock suites also support the observed differences. In suite 1 granitoids the magmatic inherited cores (433 Ma) prevailed, while only two inherited cores pointing to ages of ca. 2659–2530 Ma were found. In suite 2 leucogranites the inherited zircon crystals, showing ages older than Variscan, form a population with a broad spectrum of inherited core ages (1780–387 Ma). Such variation can be expected in melts derived from mainly metasedimentary precursors and are reconciled with crustal heterogeneity.

In low temperature melts the zircon solubility is consequently low and most of the pre-existing zircon crystals might remain undissolved. This allows preservation of the inherited components (Scott et al. 2011), but it does not explain why no new overgrowths were formed on pre-existing zircon crystals. Additionally, the presence of older, inherited components required the assimilation of the country rocks. That opens the problem of the energy, necessary for the assimilation. Whatever is the mechanism of assimilation: the mechanical disintegration or chemical dissolution, it is an energy-consuming process, resulting in a considerable degree of crystallization, what makes the magma relatively immobile (Clemens & Stevens 2012). On the other hand, if the magma brings enough heat and vapour pressure for country rocks assimilation and contamination (e.g. by MASH process = Melting, Assimilation, Storage and Homogenization, supposed to occur during deep-seated melting), the partial corrosion of the older zircon crystals should be observed, followed by later magmatic overgrowths, as is commonly noted (e.g. Gawęda 2008; Burda & Klötzli 2011). Such a process can be avoided when inherited zircon crystals (J2 and S22 in the morphology diagram) are sheltered by the so-called resister minerals (biotite, opaques, etc.; Chappell et al. 1987; Burda & Gawęda 2009), which are, however, absent in the case of suite 2. In that case, to explain the presence of a population of 387 Ma zircon crystals we assume the suite 2 represent the trapped magma portions, possibly associated with disintegrated (exploded?) xenoliths (e.g. Gawęda 2007; Gawęda & Szopa 2011), which possibly crystallized in disequilibrium conditions. That could explain the presence of graphic intergrowths of K-feldspars and quartz, typical of disequilibrium growths and also the lack of corrosion/overgrowths on the 387 Ma zircon crystals.

Another aspect of inherited zircon presence could be visible in REE fractionation, which is anomalously low in leucogranites of suite 2 (Fig. 4, Table 4). In case of the anatectic melts flat REE patterns can be caused by the resister minerals, like apatite consuming mainly LREE and zircon carrying mainly HREE (e.g. Burda & Gawęda 2009).

## Conclusions

1. The presented geochemical and geochronological results indicate that both granitoid suites, present in the Goryczkowa and Małołączniak crystalline cores in the Western Tatra Mountains, were formed in a VAG (volcanic arc granites) tectonic setting, however, they represent two different magmatic stages. Suite 1 granitoids were formed as a result of melting of amphibolite and/or mafic pelite, possible during high temperature pre-plate collisional stage and intruded at ca. 371 ± 6 Ma. Suite 2 leucogranites represent melts generated by muscovite-dehydration melting of felsic pelites during late orogenic/anatectic event and intrusion at ca. 350 ± 5 Ma.

2. The presence of magmatic U-Pb zircon ages around 387 Ma supports the existence of a LP-HT partial melting episode in the Tatra Mountains crystalline core in the Early Devonian, predating the granitoid emplacement.

3. The abundance of inherited zircon crystals, primitive trace elements chemistry, together with disequilibrium-related rock structures, could be interpreted as a result of perturbation in the crystallization course (undercooling, viscosity increase, disequilibrium crystallization). That brings an additional question about the reliability of temperature calculation based on Zr content and importance of the REE diagrams interpretation in contaminated magmas.

4. The Goryczkowa type granitoids represent the same magmatic episode and similar petrographical/geochemical characteristics as described from Western Tatra Mountains so distinguishing the Goryczkowa type as a separate type of granite is not necessary.

5. The presence of inherited zircon cores, dated ca. 430–410 Ma, in both granitoid suites, is a trace of the Avalonia–Baltica collision, and suggests that melting of the Laurussia continental crust participated in granitoid magma formation.

**Acknowledgments:** The Polish Ministry of Sciences and Higher Education sponsored the investigations, by MNiSW Grant No. 2 P04D 003 29 (given to JB) and MNiSW Grant No. N 307 027837 and DEC-2012/07/B/ST10/04366 (given to AG). Additional funds from Austrian Science Fund FWF (START Project 267-N11 and Project P18202-N10 given to UK) is deeply acknowledged. Ewa Teper MSc is thanked for the assistance during CL investigations, while Piotr Dzierżanowski PhD and Mrs Lidia Jeżak are thanked for their help during microprobe work. Comments provided by the journal reviewers to anonymous referee, Milan Kohút and Monika Kusiak are gratefully acknowledged.

## References

Bac-Moszaszwili M. 1996: The uplift of the Tatra massif in Tertiary and Quaternary. In: *The Tatra National Park – Nature and man*. Zakopane, Oct. 6th–9th 1995, Conference proceedings, 68–71.

Balintoni I., Balica C., Ducea M.N., Chen F., Hann H.P. & Sabliovschi V. 2009: Late Cambrian-Early Ordovician Gondwanan terranes in the Romanian Carpathians: a zircon U-Pb provenance study. *Gondwana Res.* 16, 119–133.

Balintoni I., Balica C., Ducea M.N., Zaharia L., Chen F., Cliveti M., Hann H.P., Li L-Q. & Ghergari L. 2010: Late Cambrian-Ordovician northeastern Gondwana terranes in the basement of the Apuseni Mountains, Romania. *J. Geol. Soc. London* 167, 1131–1145.

Batchelor R.A. & Bowden P. 1985: Petrogenetic interpretation of granitoid rock series using multicationic parameters. *Chem. Geol.* 48, 43–55.

Blundy J.D. & Holland T.J.B. 1990: Calcic amphibole equlibria and a new amphibole-plagioclase geothermometer. *Contr. Mineral. Petrology* 104, 208–244.

Broska I. & Petrík I. 2011: Accessory Fe-Ti oxides in the West-Carpathian I-type granitoids: witnesses of the granite mixing and late oxidation processes. *Miner. Petrology* 102, 87–97.

Broska I., Petrík I., Be'eri-Shlevin Y., Majka J. & Bezák V. 2013: Devonian/Mississippian I-type granitoids in the Western Carpathians: A subduction-related hybrid magmatism. *Lithos* 162–163, 27–36.

Burchart J. 1968: Rubidium-strontium isochron ages of the crystalline core of the Tatra Mountains, Poland. *Amer. J. Sci.* 266, 10, 895–907.

Burchart J. 1970: Rocks of the Goryczkowa "crystalline island" in the Tatra Mountains. [Skały krystaliczne wyspy Goryczkowej w Tatrach.] *Stud. Geol. Pol.* 32, 7–183 (in Polish).

Burda J. 2010: Internal structures and dating of complex zircons from High Tatra massif granodiorites, Poland. *10th International conference — Methods of absolute chronology, 22–25 April Gliwice*, Poland, Abstracts & Programme, 79.

Burda J. & Gawęda A. 2009: Shear-influenced partial melting in the Western Tatra metamorphic complex: geochemistry and geochronology. *Lithos* 110, 373–385.

Burda J. & Klötzli U. 2007: LA-MC-ICP-MS U-Pb zircon geochronology of the Goryczkowa type granite — Tatra Mts., Poland. *Pol. Tow. Mineral. Prace Spec.* 31, 89–92.

Burda J. & Klötzli U. 2011: Pre-Variscan evolution of the Western Tatra Mountains: new insights from U-Pb zircon dating. *Miner. Petrology* 102, 99–115.

Burda J., Gawęda A. & Klötzli U. 2011: Magma hybridization in the Western Tatra Mountains granitoid intrusion (S-Poland, Western Carpathians). *Miner. Petrology* 103, 19–36.

Burda J., Gawęda A. & Klötzli U. 2013: U-Pb zircon age of the youngest magmatic activity in the High Tatra granites (Central Western Carpathians). *Geochronometria* 40, 2, 134–144.

Chappell B.W., White A.J.R. & Wyborn D. 1987: The importance of residual source material (restite) in granite petrogenesis. *J. Petrology* 28, 6, 1111–1138.

Clemens J.D. & Stevens G. 2012: What controls chemical variation in granitic magmas? *Lithos* 134–135, 317–329.

De la Roche H., Leterrier J., Grandclaude P. & Marchal M. 1980: A classification of volcanic and plutonic rocks using $R_1$,$R_2$-diagrams and major element analysis — its relationships with current nomenclature. *Chem. Geol.* 29, 183–210.

Finger F., Roberts M.P., Haunschmid B., Schermaier A. & Steyrer H.P. 1997: Variscan granitoids of Central Europe: their typology, potential sources and tectonothermal relations. *Miner. Petrology* 61, 67–96.

Frost B.R. & Frost C.D. 2008: A geochemical classification for feldspathic igneous rocks. *J. Petrology* 49, 1955–1969.

Gaab A.S., Poller U., Todt W. & Janák M. 2003: Geochemical and isotopic characteristics of the Muráň gneiss complex, Veporic unit (Slovakia). *J. Czech Geol. Soc.* 48, 52.

Gawęda A. 2001: Alaskites of the Western Tatra Mountains: A record of Early-Variscan collisional stage in the Carpathians pre-continent. *Univ. Silesia Publ. House, Monograph. Ser., 1997*, Katowice, 1–142 (in Polish, English abstract).

Gawęda A. 2007: Mega-xenolith from Velicka Valley (High Tatra Mountains, Western Carpathians): an example of exploding elephant. *Pol. Tow. Mineral. Prace Spec.* 31, 115–118.

Gawęda A. 2008: Apatite-rich enclave in the High Tatra granite, Western Carpathians: petrological and geochronological study. *Geol. Carpathica* 59, 4, 295–306.

Gawęda A. 2009: Enclaves in the High Tatra Granite. *Univ. Silesia Publ. House, Monograph. Ser., 2637*, Katowice, 1–180 (in Polish, English abstract).

Gawęda A. & Golonka J. 2011: Variscan plate dynamics in the Circum-Carpathian area. *Geodin. Acta* 24, 3–4, 141–155.

Gawęda A. & Szopa K. 2011: The origin of magmatic layering in the High Tatra granite, Central Western Carpathians — implications for the formation of granitoid plutons. *Earth Env. Sci. T. R. So.* 102, 129–144.

Gawęda A., Doniecki T., Burda J. & Kohút M. 2005: The petrogenesis of quartz-diorites from the Tatra Mountains (Central Western Carpathians): an example of magma hybridisation. *Neu. Jb. Miner. Abh.* 181, 1, 95–109.

Gawęda A., Winchester J.A., Kozłowski K., Narębski W. & Holland G. 2000: Geochemistry and paleotectonic setting of the amphibolites from the Western Tatra Mountains. *Geol. J.* 35, 69–85.

Janák M., Finger F., Plašienka D., Petrík I., Humer B., Méres Š. & Lupták B. 2002: Variscan high P-T recrystallization of Ordovician granitoids in the Veporic unit (Nízke Tatry Mountains, Western Carpathians): new petrological and geochronological data. *Geolines* 14, 38–39.

Jaroszewski W. 1965: Geological structure of the upper part of Kościeliska Valley in the Tatra Mts. *Acta Geol. Pol.* 15, 4 (in Polish, English abstract).

Jurewicz E. 2006: Petrophysical control on the mode of shearing in the sedimentary rocks and granitoid core of the Tatra Mountains during Late Cretaceous nappe-thrusting and folding, Carpathians, Poland. *Acta Geol. Pol.* 56, 2, 159–170.

Kemp A.I.S. & Hawkesworth J. 2005: Granitic perspectives on the generation and secular evolution of the continental crust. In: Rudnick R. (Ed.): The crust — Treatise on geochemistry 3. *Elsevier*, Amsterdam, 349–410.

Klötzli U., Klötzli E., Günes Z. & Košler J. 2009: External accuracy of laser ablation U-Pb zircon dating: results from a test using five different reference zircons. *Geostand. Geoanal. Res.* 33, 1, 5–15.

Kohút M. & Janák M. 1994: Granitoids of the Tatra Mts, Western Carpathians: Field relations and petrogenetic implications. *Geol. Carpathica* 45, 5, 301–311.

Kohút M. & Siman P. 2011: The Goryczkowa granitic type — SHRIMP dating of an original granodiorite-tonalite variety. *Mineralogia, Spec. Pap.* 38, 113–114.

Kohút M., Poller U., Gurk C. & Todt W. 2008: Geochemistry and U-Pb detrital zircon ages of metasedimentary rocks of the Lower Unit, Western Tatra Mountains (Slovakia). *Acta Geol. Pol.* 58, 371–384.

Kohút M., Madarás J. & Siman P. 2009: Centenary of the Goryczkowa granite type (Tatra Mts.): The myth and reality. *Geovestník, 8thAnn. Seminary of the Slovak Geol. Soc.*, 550–551.

Kohút M., Uher P., Putiš M., Broska I., Rodionov N. & Sergeev S. 2010: Are there any differences in age of the two principal Variscan (I- & S-) granite types from the Western Carpathians? — a SHRIMP approach. In: Kohút M. (Ed.): Dating of minerals and rocks, metamorphic, magmatic and metallogenetic processes, as well as tectonic events. *State Geol. Inst. Dionýz Štúr*, Bratislava, 17–18.

Ludwig K.R. 2003: Isoplot/Ex version 3.00. A geochronological toolkit for Microsoft Excel. *Berkeley Geochronology Center, Spec. Publ.,* No. 4.

Morozewicz K. 1914: Über die Tatragranite. *Neu. Jb. Miner. Geol. Paläont.* 39, 289–345.

Patiño Douce A. E. 1999: What do experiments tell us about the relative contributions of crust and mantle to the origin of granitic magmas? In: Castro A., Fernandez C. & Vigneresse J.L. (Eds.): Understanding granites: Integrating new and classical techniques. *Geol. Soc. London, Spec. Publ.* 168, 55–75.

Pearce J.A., Harris N.B.W. & Tindle A.G. 1984: Trace elements discrimination diagram for the tectonic interpretation of granitic rocks. *J. Petrology* 25, 4, 956–983.

Pecerillo A. & Taylor S.R. 1976: Geochemistry of Eocene calc-alkaline volcanic rocks from the Kastamonu area, northern Turkey. *Contr. Mineral. Petrology* 58, 63–81.

Poller U. & Todt W. 2000: U-Pb single zircon data of granitoids from the High Tatra Mountains (Slovakia): implications for the geodynamic evolution. *Trans. Roy. Soc. Edin-Earth* 91, 235–243.

Poller U., Janák M., Kohút M. & Todt W. 2000: Early Variscan magmatism in the Western Carpathians: U-Pb zircon data from granitoids and orthogneisses of the Tatra Mountains, Slovakia. *Int. J. Earth Sci.* 89, 336–349.

Poller U., Todt W., Kohút M. & Janák M. 2001: Nd, Sr, Pb isotope study of the Western Carpathians: implications for the Paleozoic evolution. *Schweiz. Mineral. Petrogr.* 81, 159–174.

Pupin J.P. 1980: Zircon and granite petrology. *Contr. Mineral. Petrology* 73, 207–220.

Putiš M., Ivan P., Kohút M., Spišiak J., Siman P., Radvanec M., Uher P., Sergeev S., Larionov A., Méres Š., Demko R. & Ondrejka M. 2009: Meta-igneous rocks of the West-Carpathian basement, Slovakia: indicators of Early Paleozoic extension and shortening events. *Bull. Soc. Geol. France* 180, 6, 461–471.

Ridolfi F., Renzulli A. & Puerini M. 2010: Stability and chemical equilibrium of amphibole in calc alkaline magmas: an overview, new thermometric formulations and application to subduction-related volcanoes. *Contr. Mineral. Petrology*, 160, 45–66. Doi: 10.1007/s00410-009-0465-7

Schmidt M.W. 1992: Amphibole equilibria in tonalite as a function of pressure: an experimental calibration of the Al-in-hornblende barometer. *Contr. Mineral. Petrology* 110, 304–310.

Schmidt M.W. & Poli S. 2004: Magmatic epidote. *Rev. Mineral. Geochem.* 56, 399–430.

Scott J.M., Palin J.M., Cooper A.F., Sagar M.W., Allibone A.H. & Tulloch A.J. 2011: From richer to poorer: zircon inheritance in Pomona Island Granite, New Zealand. *Contr. Mineral. Petrology* 161, 667–681.

Sláma J., Kosler J., Schaltegger U., Tubrett M. & Gutjahr M. 2006: New natural zircon standard for laser ablation ICP-MS U-Pb geochronology. *Abstract WP05. Winter Conference on Plasma Spectrochemistry*, Tucson, 187–188.

Sun S.S. & McDonough W.F. 1989: Chemical and isotopical systematics of oceanic basalts: implications for mantle composition and processes. Magmatism in the Oceanic Basins. *Geol. Soc., Spec. Publ.* 42, 313–345.

Thirwall M.F., Smith T.E., Graham A.M., Theodorou N., Hollings P., Davidson J.P. & Arculus R.J. 1994: High field strength element anomalies in arc lavas: Source or process? *J. Petrology* 35, 3, 819–838.

Vavra G. 1990: On the kinematics of zircon growth and its petrogenetic significance: a cathodoluminescence study. *Contr. Mineral. Petrology* 106, 1, 90–99.

Vavra G. 1994: Systematics of internal zircon morphology in major Variscan granitoid types. *Contr. Mineral. Petrology* 117, 4, 331–344.

Watson T.M. & Harrison E.B. 1983: Zircon saturation revisited: temperature and composition effects in a variety of crustal magma types. *Earth. Planet. Sci. Lett.* 64, 295–304.

Whitney D.L. & Evans B.W. 2010: Abbreviations for names of rock-forming minerals. *Amer. Mineralogist* 95, 185–187.